YIELD AND RELAXATION
IN POLYMERIC GLASSES

Thesis for the Degree of Ph. D.
MICHIGAN STATE UNIVERSITY
ROBERT HOWARD BECK, JR.
1971

LIBRARY
Michigan State
University

This is to certify that the

thesis entitled

Yield and Relaxation in Polymeric Glasses

presented by

Robert Howard Beck, Jr.

has been accepted towards fulfillment
of the requirements for

PhD. degree in Mechanics

Terry Triffet
Major professor

Date 18 May 1971

O-169

BINDING BY
HOAG & SONS'
BOOK BINDERY INC.
BINDERS
SPRINGPORT, MICHIGAN

ABSTRACT

YIELD AND RELAXATION
IN POLYMERIC GLASSES

By

R. H. Beck, Jr.

The yield process in amorphous polymeric glasses may be a relaxation phenomenon. A combined kinetic-energy/free-volume theory for molecular mobility of polymer liquids is extended for use in the glassy state. Expressions for tensile yield strain as a function of temperature, strain rate, and time after quench during isothermal volume contraction, and for relaxation rate as a function of temperature, tensile elongation, and time after quench are derived.

Workers in the area of glassy yield generally have taken specimen necking to denote tensile yield. From measurements of the volume change undergone during extension by polymethylmethacrylate glass (PMMA), and from the dependence of the fractional hysteresis of that material upon elongation, it is shown in the present work that tensile yield initiates prior to necking, near the proportional limit of the load-elongation curve. Poisson's ratio, calculated from the volume measurements, is found to vary from 0.33 to 0.41 between -20°C and 100°C.

Results of experimental measurements of tensile yield strain and relaxation rate of PMMA as functions of temperature and free volume are shown to be consistent with a yield-relaxation relationship. Using the theory and measurements of volume change during extension,

a load-elongation curve is calculated which exhibits a distinct yield point. Though qualitatively successful in describing yield strain and relaxation rate, the theory is demonstrated to be quantitatively applicable only to yield strain calculations for strain rates within one decade of a reference rate.

YIELD AND RELAXATION
IN POLYMERIC GLASSES

By

Robert Howard Beck, Jr.

A THESIS

Submitted to
Michigan State University
in partial fulfillment of the requirements
for the degree of

DOCTOR OF PHILOSOPHY

Department of Metallurgy, Mechanics,
and Materials Science

1971

60297

ACKNOWLEDGMENTS

I should like very much to thank my thesis director, Dr. T. Triffet, for his help in the preparation of this thesis. In addition, special thanks are due the Polymer Science Department, Ford Motor Company, for its support of this work. Finally, I wish to express my deepest gratitude to Dr. K. C. Rusch for his inestimable aid during the course of this research.

TABLE OF CONTENTS

Page

LIST OF TABLES v

LIST OF FIGURES vi

LIST OF SYMBOLS ix

1. INTRODUCTION 1

    1.1 The Glassy State 1
    1.2 Polymer Relaxation 3
    1.3 The Glass Transition as a Relaxation Phenomenon . . . 6
    1.4 Yield as a Relaxation Phenomenon 7
    1.5 The Present Work 8

2. MATHEMATICAL DESCRIPTION OF YIELD AND RELAXATION 11

    2.1 Free Volume 11
    2.2 Kinetic Energy 15
    2.3 Relaxation Times 17
    2.4 Yield Strain 22
    2.5 Relaxation Rate 25

3. DETERMINATION OF INITIAL YIELD POINT 26

    3.1 Volume-Elongation Measurements 26
    3.2 Fractional Hysteresis-Elongation Measurements 28

4. YIELD AND RELAXATION MEASUREMENTS 34

    4.1 Yield Strain 34
    4.2 Relaxation Rate 38

5. COMPARISON OF THEORY AND EXPERIMENT 41

    5.1 Yield Strain 41
    5.2 Relaxation Rate 52
    5.3 Direct Yield-Relaxation Relation 58

6. DISCUSSION 61

7. CONCLUSIONS 68

8. LIST OF REFERENCES 70

TABLE OF CONTENTS (CONT.)

Page

APPENDIX 72

A. Dilatometer 72
B. Experimental Procedure for Dilatometer 75
C. Dilatometer and Hysteresis Data 77
D. BASIC Program R-Rate Used for Relaxation Rate Calculation-Temperature Dependence 82

LIST OF TABLES

Table Page

1. Yield Elongation Versus Temperature Obtained from Volume Measurements 28

2. Yield Elongation Versus Temperature Obtained from Hysteresis Measurements 32

3. Poisson's Ratio and Specific Volume for PMMA 43

4. Calculated Material Constants for PMMA for Given Values of E* 45

5. Dependence of Free Volume Upon Time After Quench . . . 48

6. T_g^* Values for Various Strain Rates 51

7. Effective Temperature for E* = 20 Kcal/mole and t_q = 1800 Seconds 51

8. Dependence of Yield Strain Upon Free Volume 52

LIST OF FIGURES

Figure Page

1. Schematic drawing of a cooling curve for a typical amorphous polymer 2

2. Schematic drawing of cooling curves, showing the rate dependence of the glass-transition temperature and glass volume 3

3. Schematic drawing of a typical stress-relaxation curve 4

4. Series of stress-relaxation curves for PMMA 5

5. Stress-relaxation master curve constructed using data given in Figure 4 6

6. Schematic drawing of tensile load-elongation curve showing upper yield point, ε_B 9

7. Experimental specific volume-temperature curve for PMMA 13

8. Tensile-extension dilatometer data for PMMA for T = 60°C 27

9. Strain-time diagram for constant-frequency, single-cycle load-elongation experiment. 29

10. Fractional hysteresis data for PMMA for T = 20°C . . . 32

11. Tensile-test specimen configuration 35

12. Yield strain of PMMA as a function of temperature and strain rate 35

13. Schematic drawing showing method of yield point determination for a flexural test 37

14. Yield strain of PMMA as a function of time after quench 37

15. Ten-second relaxation rate of PMMA as a function of temperature 38

LIST OF FIGURES (CONT.)

Figure Page

16. Ten-second relaxation rate of PMMA as a function of applied elongation 39

17. Ten-second relaxation rate of PMMA as a function of time after quench for T = 30°C 40

18. Ten-second relaxation rate of PMMA as a function of time after quench for T = 50°C 40

19. Poisson's ratio of PMMA as a function of temperature 42

20. Log a_T of PMMA as a function of temperature for $t_q = 10^4$ seconds 43

21. $V_t - V_\infty$ of PMMA as a function of temperature for $t_q = 10^4$ seconds 44

22. Series of stress-relaxation curves for PMMA for various times after quench for T = 70°C 47

23. Log a_T of PMMA as a function of time after quench for T = 70°C 47

24. $-(\partial \log a_T/\partial V_f)_T$ of PMMA as a function of temperature; points are experimental data and lines are calculated from the theory 49

25. Yield strain of PMMA as a function of temperature for $\dot{\varepsilon} = 1.2\%$/second and theoretical curves for various values of E* 49

26. Yield strain of PMMA as a function of temperature and theoretical curves for E* = 20 Kcal/mole . 50

27. Relaxation spectrum used in integration of Eq. (33). 53

28. Ten-second relaxation rate of PMMA as a function of temperature and theoretical curve 55

29. Ten-second relaxation rate of PMMA as a function of applied elongation and theoretical curves . . . 56

30. Ten-second relaxation rate of PMMA as a function of time after quench for T = 30°C and theoretical curve 57

LIST OF FIGURES (CONT.)

Figure Page

31. Ten-second relaxation rate of PMMA as a function of time after quench for T = 50°C and theoretical curve 58

32. Experimental and calculated load-elongation curves for PMMA for T = 60°C 60

33. Schematic drawing of tensile-extension dilatometer . 72

34. Tensile-extension dilatometer specimen 73

35. Tensile-extension dilatometer data for PMMA for T = -20°C 77

36. Tensile-extension dilatometer data for PMMA for T = 0°C 78

37. Tensile-extension dilatometer data for PMMA for T = 20°C 78

38. Tensile-extension dilatometer data for PMMA for T = 40°C 79

39. Tensile-extension dilatometer data for PMMA for T = 80°C 79

40. Tensile-extension dilatometer data for PMMA for T = 100°C 80

41. Fractional hysteresis data for PMMA for T = 0°C 80

42. Fractional hysteresis data for PMMA for T = 40°C 81

43. Fractional hysteresis data for PMMA for T = 60°C 81

LIST OF SYMBOLS

A	cross-sectional area of specimen
C_1, C_2	constants used to fit WLF equation
E	tensile modulus
E*	potential energy barrier to molecular transition
F	force
H	relaxation-time distribution function
K	spring constant
P_E	energy probability for molecular transition
P_T	total probability for molecular transition
$P_{T_{cr}}$	critical probability for molecular transition
P_V	volume probability for molecular transition
PMMA	polymethylmethacrylate
R	gas constant
T	temperature
T_e	effective temperature
T_g	glass transition temperature
T_g^*	critical temperature
T_o	WLF reference temperature
T_2	true second-order thermodynamic transition temperature
V	volume
V_f	total free volume
V_c	occupied volume

LIST OF SYMBOLS (CONT.)

V^*	critical volume
V_o	initial volume (unstrained)
V_∞	volume of glass if cooling curve followed liquid line
W	fractional hysteresis

a_T	WLF shift factor
f	fractional free volume (after Ferry and Stratton)
t	time
t_q	time after quench from temperature above the glass transition temperature to one below
t_o	half-cycle time for hysteresis experiments
v_f	equilibrium free volume
w_f	nonequilibrium free volume
x	extension of Maxwell element

α_c	thermal-expansion coefficient of completely crystalline state (after Litt)
α'_c	slope of cooling curve for completely crystalline state
α'_g	slope of cooling curve for glass
$\alpha'_{g(t\to\infty)}$	slope of cooling curve for glass for infinitely slow cooling rate
α'_ℓ	slope of cooling curve for liquid
β	free-volume correspondence factor (after Ferry and Stratton)
γ	volume overlap factor (after Cohen and Turnbull)
$\Delta\alpha_f$	$\alpha'_\ell - \alpha'_{g(t\to\infty)}$

LIST OF SYMBOLS (CONT.)

ε	tensile strain
ε_A	strain at initial yield
ε_B	strain at tensile load-elongation curve maximum
ε_t	strain transverse to ε
ε_y	yield strain
ε_o	strain applied for stress-relaxation experiment; maximum strain applied for hysteresis experiment
η	viscosity
μ	Poisson's ratio
ρ	density
σ	stress
τ	relaxation time

1. INTRODUCTION

Although amorphous polymeric glasses are generally thought of as brittle, such materials do, under certain conditions, yield and draw without undergoing brittle fracture. Much attention has been given to the phenomenon of glassy yield,[1-12] especially experimentally, but with little quantitative agreement between experimental results and theoretical predictions. The purpose of the present work is to investigate yield in tension of polymethylmethacrylate glass (PMMA),* a typical amorphous polymeric glass, and to describe quantitatively the tensile yield process for that material in particular, and amorphous polymeric glasses in general.

1.1 The Glassy State

As an amorphous polymer in the liquid state is cooled, its volume decreases. The slope of the specific volume-temperature curve is designated α'_ℓ (Figure 1). At some temperature, the slope of the cooling curve begins to decrease, and over a temperature range of about 30°C becomes constant at a lower value, α'_g. In the region in which the cooling curve slope is constant and less than for the liquid, the polymer is in the glassy state. The temperature at which the slope changes (found by the intersection of the extrapolated liquid and glass lines) is called the glass-transition temperature, T_g. At temperatures greater than T_g, the polymer behaves as a viscous liquid, and below T_g it acts as a rigid, viscoelastic solid. Typical polymers which are glasses at room temperature are polystyrene, polycarbonate, and PMMA.

---

*American Cyananid Acrylite MS-2; MIL-P-5425A, Finish A

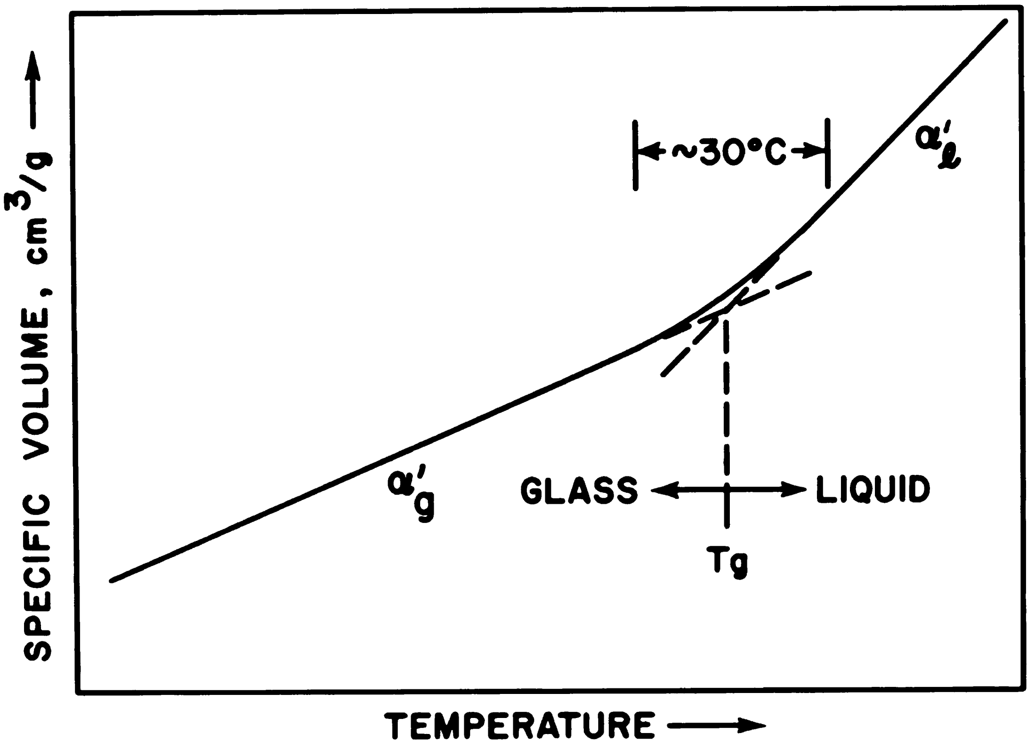

Figure 1--Schematic drawing of a cooling curve for a typical amorphous polymer.

The glass transition is rate-dependent, as is illustrated by Figure 2, which shows schematic volume-temperature curves for three cooling rates. The figure shows that the volume of the glass is rate-dependent also; both the glass-transition temperature and the glass volume decrease with decreasing cooling rate. The rate dependence of the volume is a manifestation of the nonequilibrium character of the glassy state. If the polymer were cooled infinitely slowly, the rate-controlled glass transition would occur at the true second-order thermodynamic transition temperature, T_2 (Figure 2).[13, 14, 15] The state resulting from such cooling is called the hypothetical-equilibrium glass and the slope of the associated glass curve is designated $\alpha'_{g(t\rightarrow\infty)}$.[13] The hypothetical-equilibrium glass is that state in which total polymer volume

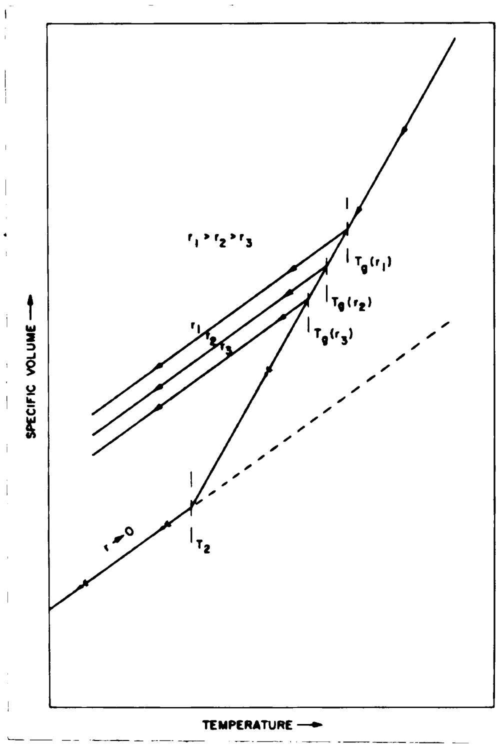

Figure 2--Schematic drawing of cooling curves, showing the rate dependence of the glass-transition temperature and glass volume.

is made up only of the sum of the volume of the molecules themselves and the volume characteristic of their thermal vibrations. If the glass exists in any state other than this, it contains excess volume over and above the hypothetical-equilibrium volume. The explanation for this phenomenon will be given in a subsequent section.

1.2 Polymer Relaxation

If a strain ε_o is applied very rapidly to a polymer, and the force necessary to maintain that strain monitored as a function of time, a curve similar to that of Figure 3 results, where the log of the apparent modulus, E(t), is plotted versus log time. The figure shows that E(t) decreases with time, indicating that the force needed to

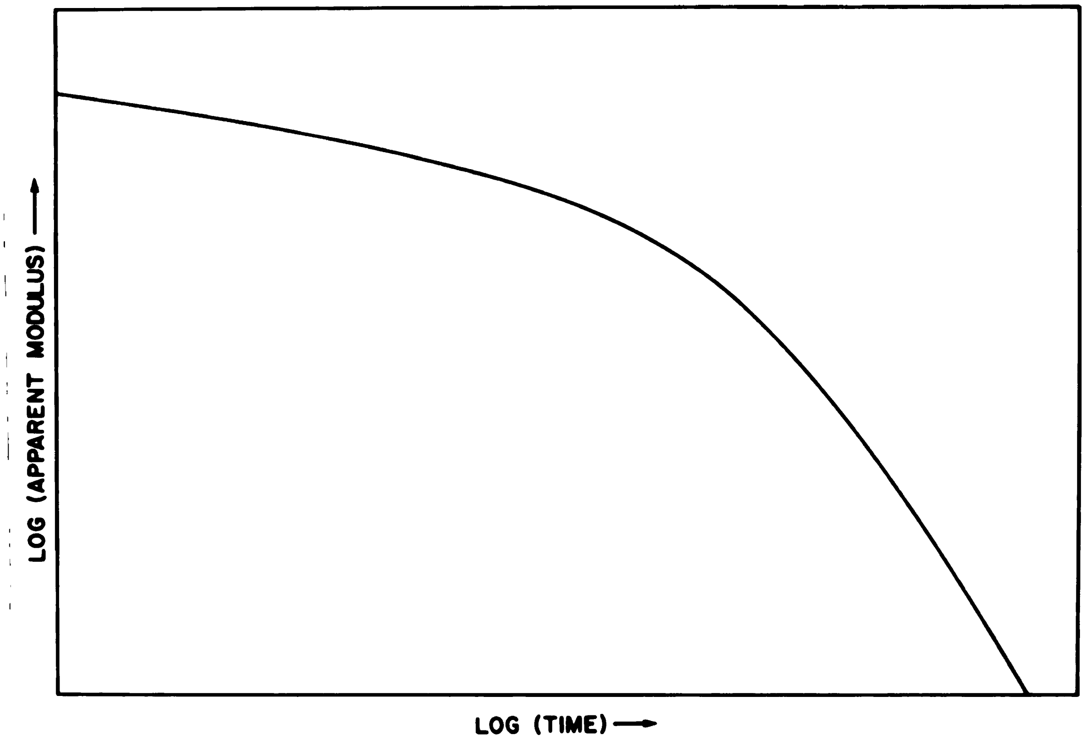

Figure 3--Schematic drawing of a typical stress-relaxation curve.

maintain strain ε_o decreases. It is said that the polymer relaxes. The rate of relaxation is given by the negative of the slope of the curve, $(-\partial \log E(t)/\partial \log t)_{T,\varepsilon}$ at any given time. A high rate indicates greater mobility of the polymer molecules, or chains, than does a low rate. It is said that a polymer which relaxes quickly has short relaxation times. The meaning of the term "relaxation time" will be made clear later.

Relaxation of the stress during such a test occurs as a result of polymer chains' changing configuration under the influence of the stress; such a test is called a stress-relaxation experiment. A series of tests run over a range of temperatures for PMMA is shown in

Figure 4.[16] A particular modulus may be realized in two ways: by choosing the test temperature where the initial modulus is suitable, or by testing at a lower temperature but waiting for a longer time--until the modulus is lowered by relaxation.

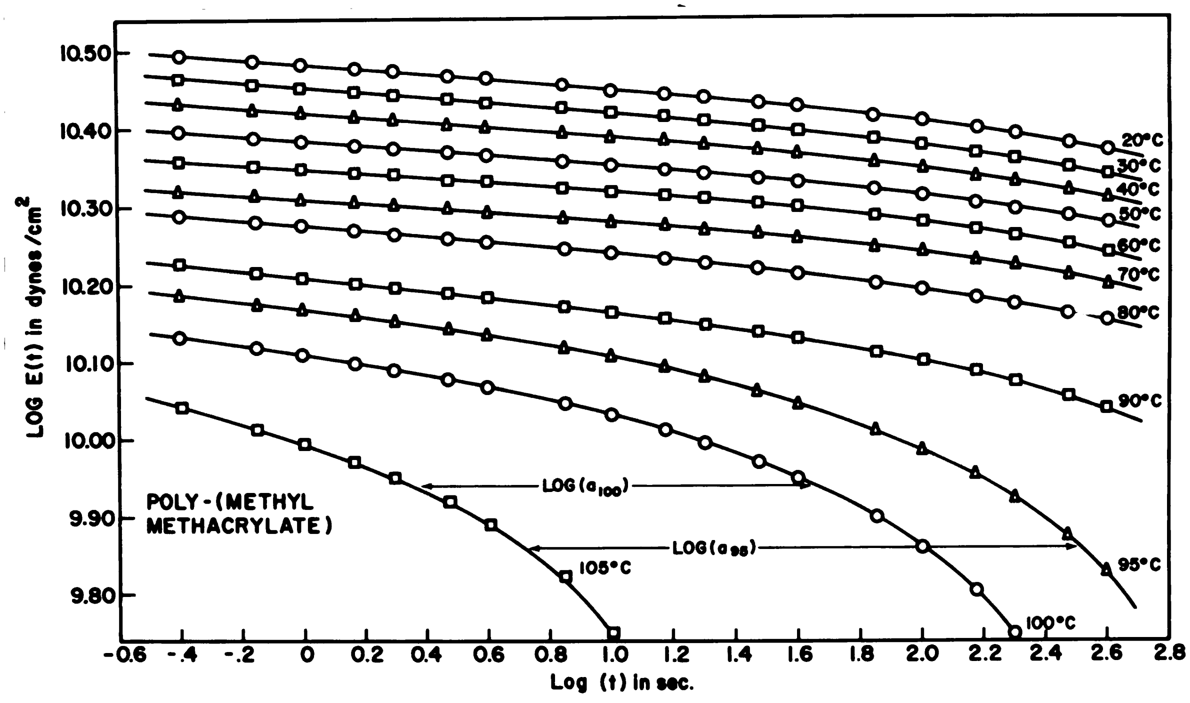

Figure 4--Series of stress-relaxation curves for PMMA.

The equivalence of time and temperature is the qualitative basis of the time-temperature superposition principle,[17] which states that the effect of changing the temperature of a polymer is equivalent to changing the time scale of the experiment. The most important parameter in the theory of time-temperature superposition is the shift factor, a_T. The shift factor is a measure of the time-temperature equivalence. It is obtained experimentally by superimposing stress-relaxation curves for the various temperatures, to make a single "master curve." A master curve constructed using the data of Figure 4 is shown below. The amount of horizontal shift, as measured on the log t axis, necessary to produce the master curve is log a_T. Log a_T is a function of temperature and is illustrated in Figure 4 for 95°C and 100°C, where the shift reference temperature, T_o, is 105°C.

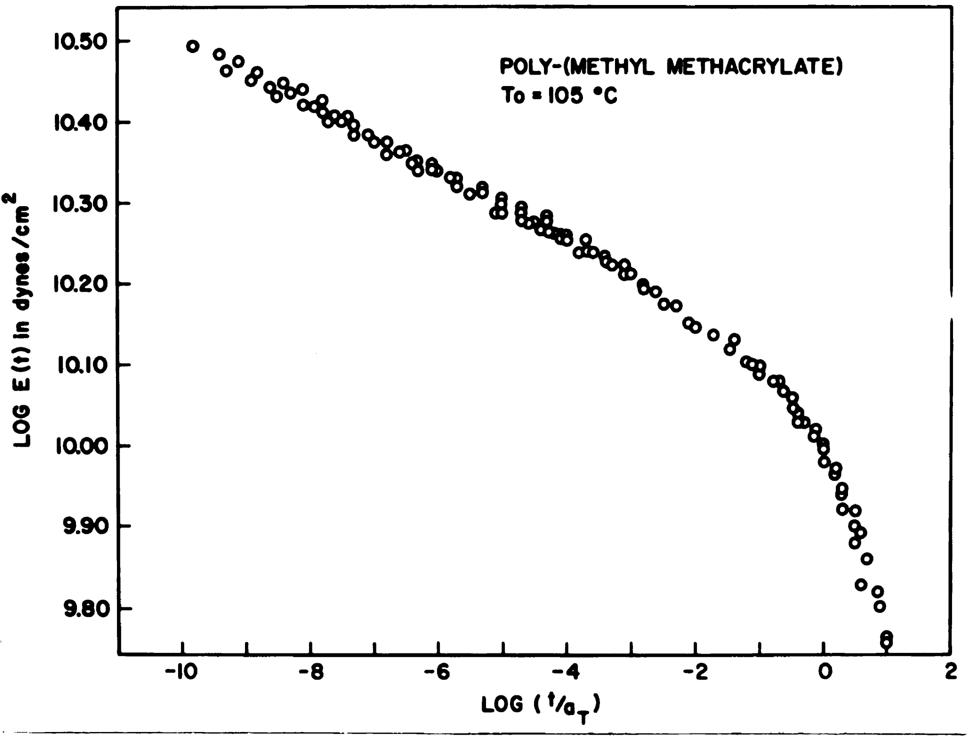

Figure 5--Stress-relaxation master curve constructed using data given in Figure 4.

1.3 The Glass Transition as a Relaxation Phenomenon

The glass transition is known to be relaxational in nature.[15,18,19] As the polymer in the liquid state is cooled, the temperature change causes the molecular segments to alter their configuration and increase the density of the polymer. Figure 4 shows that the mobility of the polymer chains decreases with decreasing temperature. This is evidenced by the lowering of relaxation rate with lowering of temperature.

Sometime during the cooling, a temperature is reached where the chains are no longer able to respond at a rate equal to the cooling rate, owing to their decreased mobility, and volume change begins to lag temperature change. At that point the slope of the cooling curve begins to decrease (Figure 1), since the chains are not responding as rapidly as at higher temperatures. The slope continues to decrease, over a range of about 30°C, until the relaxation rate is so small compared with the cooling rate that an apparent steady state results. The slope then appears constant. As a result of the temperature dependence of polymer mobility, the point at which the glass transition occurs is dependent upon cooling rate. The glass-transition temperature shifts about 3°C for a one-decade change in rate.

1.4 Yield as a Relaxation Phenomenon

Analogously, yield in amorphous glasses is believed to be relaxationally controlled. At small strains, the glass behaves as a viscoelastic solid with long relaxation times (low chain mobility), and reacts in a very nearly Hookean manner. The imposition of increasing strain on the glass alters its character and has the effect of shortening relaxation times. At some time during the loading, it is surmised that chain mobility will have been increased to the point where the relaxation rate of the glass is equivalent to the rate of strain imposition, and that the glass responds within the time scale of the test by yielding. At yield, the material acts as if a very low stress were imposed upon it, but at a temperature quite near T_g. That is, it behaves as if it were liquid-like in character. Possibly as a result of the relaxational aspect of yield, the point at which yield occurs changes with strain rate, similar to the cooling-rate shift of T_g. The yield point also changes with temperature. This would occur as a result of the temperature dependence of the relaxation rate. As the test temperature is increased, the relaxation rate in the unstrained state is also increased, and the amount of strain necessary to increase the relaxation rate to equivalence with the strain rate would be lowered. Thus the yield strain may be expected to decrease with increasing temperature.

1.5 The Present Work

The main objective of the present work is to investigate the possibility that yield in polymeric glasses is a relaxational phenomenon, as described above. It has been stated that applied strain increases relaxation rate, thus causing yield. The first portion of the present work will be concerned with the development of a mathematical description for this proposed type of yield behavior.

The model itself is based upon the free-volume theory of molecular mobility, according to which the rate of relaxation of a polymer increases with increasing free volume. Equations for the probability of a molecular transition, originally derived for the liquid state, will be extended for use in the glassy state. It is hypothesized that when the transitional probability of the glass reaches $P_{T_{cr}}$, the "critical transitional probability," yield occurs. An expression for $P_{T_{cr}}$, which is dependent upon temperature and free volume, will be developed. Quantitative relations will also be obtained for yield strain and relaxation rate as a function of temperature and free volume.

In the area of glassy yield, it has been customary for workers[1-12] measuring the yield point of a polymer to take the maximum in the tensile load-elongation curve to denote yield (ε_B in Figure 6). This is also the point at which necking is first observed, and although the existence of a neck in the specimen provides certain evidence of yield, the macroscopic character of the plastic deformation at that point makes it equally certain that yield must have initiated at some prior point. It would seem that any theory devised to describe yield should predict its onset, and therefore must utilize experimental data taken at yield initiation, rather than at necking. One portion of this work will address itself to the problem of experimentally determining the initial yield point.

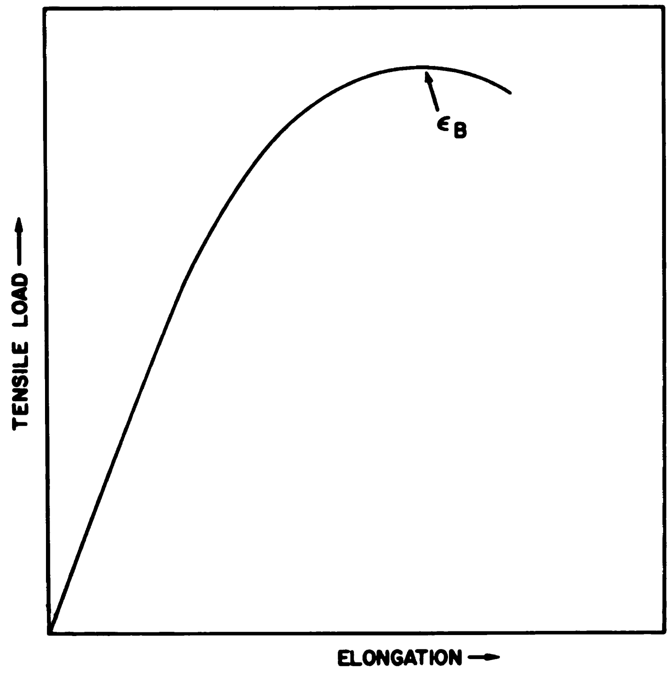

Figure 6--Schematic drawing of tensile load-elongation curve showing upper yield point, ε_B.

With the yield point properly defined, experiments will be reported whereby the variation of initial yield strain with temperature,

strain rate, and free volume were determined. Measurements showing the dependence of relaxation rate upon applied strain and free volume will also be described.

Results of the experiments will be compared with predictions based upon the mathematical model, and final conclusions will then be drawn.

2. MATHEMTICAL DESCRIPTION OF YIELD AND RELAXATION

To determine quantitatively whether glassy yield in amorphous polymers is relaxation in nature, it is necessary to have a mathematical model for yield and relaxation. Such a model must include a strain-induced relaxation rate increase and must relate that change in relaxation rate to the yield point.

2.1 Free Volume

The basis of the model presented here is the free-volume theory of molecular mobility. First introduced by Doolittle,[20] and Williams, Landel, and Ferry[17] to describe the temperature dependence of polymer viscosity above the glass transition, the theory has since been extended empirically by other workers[6-9] to describe glassy yield. These efforts have met with only moderate success. According to the theory, molecular mobility is directly related to the amount of free volume in the polymer; increases in free volume increase mobility. In the glassy state, it is presumed that the volume increase which accompanies tensile deformation constitutes a change in free volume, thus increasing mobility.

Free volume is not the only parameter on which the development of a yield theory could be based. Entropy[18] or heat capacity, for instance, might be used instead. An approach in which a parameter other than free volume is used may seem more desirable from a theoretical point of view. Experimentally, however, it is much easier to measure volume precisely than entropy or heat capacity, and hence the former approach is taken in this work.

The thermal expansion of a polymer consists of two parts: free volume, V_f, and occupied volume, V_c. Occupied volume corresponds to the volume of the hypothetical-equilibrium glass. The free volume is defined as that part of the thermal expansion which is "free" for redistribution,[21] and in the glassy state may be thought of as being composed of an equilibrium component, v_f, and a nonequilibrium, or "frozen," component, w_f.[13] There is no physical difference between v_f and w_f. The distinction is made because w_f represents that portion of the total free volume which will relax out of the polymer, given a sufficiently long period of time, whereas v_f represents the value of the total free volume at thermodynamic equilibrium.

The components of V_f are illustrated on the volume-temperature diagram for PMMA shown in Figure 7. This shows that the temperature dependence of equilibrium free volume is: $v_f = \Delta\alpha_f(T - T_2)$, where $\Delta\alpha_f = \alpha'_\ell - \alpha'_{g(t\to\infty)}$. The value of w_f is a function of the thermal history of the glass.

The basis of the free-volume theory is the assumption that the probability of a molecular segment's making a transition, or jump, from one equilibrium position to another depends solely upon the probability of the existence of a "hole" of sufficient size such that the segment can fit into it. Cohen and Turnbull[21] calculated the probability, P_V, of the existence of a hole of volume equal to or greater than some value V*, on the basis of a hard-sphere model, and found

$$P_V \propto \exp(-\gamma V^*/V_f) \qquad (1)$$

where γ is a factor between 0.5 and 1, and which is needed to correct for overlap of free volume. Rusch[13] has shown that $\gamma V^* = 2.303 C_1 C_2 \Delta\alpha_f$, and $C_2 = T_o - T_2$.

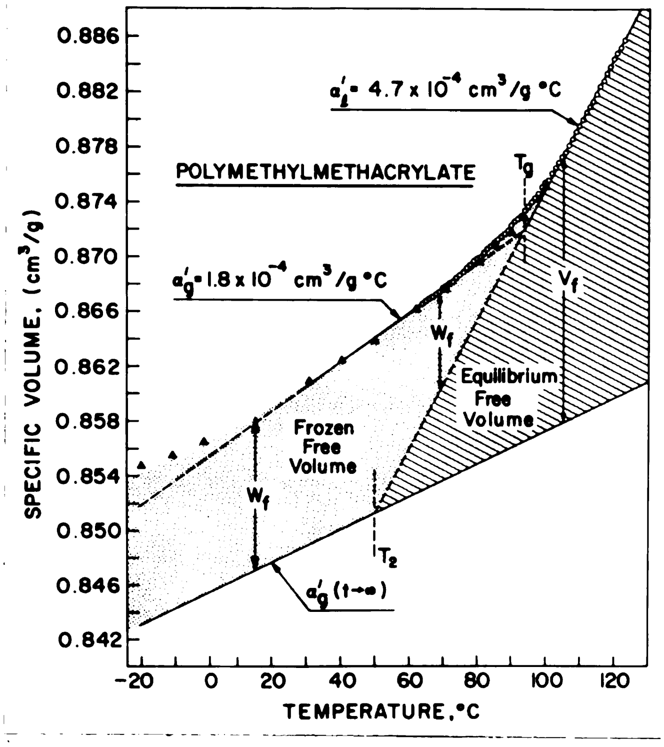

Figure 7--Experimental specific volume-temperature curve for PMMA.

When a material is subjected to a tensile strain, ε, a volume increase generally accompanies the strain. The amount of volume increase is given by

$$\frac{\Delta V}{V_o} = (1 + \varepsilon)^{1-2\mu} - 1 \tag{2}$$

where ΔV is the volume change, V_o is the volume at zero strain, and μ is Poisson's ratio, defined by

$$\mu = \frac{-\ln(1 + \varepsilon_t)}{\ln(1 + \varepsilon\ )} \tag{3}$$

with ε_t indicating the strain in a direction transverse to ε. For small strains the above equations reduce to

$$\frac{\Delta V}{V_o} = \varepsilon(1 - 2\mu) \tag{4}$$

and

$$\mu = \frac{-\varepsilon_t}{\varepsilon}. \tag{5}$$

Materials for which $\mu = 0.5$ deform at constant volume (as do liquids).

In extending the theory to glassy yield, Ferry and Stratton[6] pointed out that the volume increase resulting from the application of a tensile stress could be assumed proportional to an increase in the fractional free volume, f, and proposed the relation

$$\frac{\partial f}{\partial \varepsilon} = \beta(1 - 2\mu) \tag{6}$$

where β is a constant which denotes the fraction of total volume dilation which is free volume. Newman and Strella[7] equated this volume dilation to that which results from a temperature increase. Setting $\beta = 1$, they suggested the relation

$$\varepsilon(1 - 2\mu) = \alpha_g \Delta T \tag{7}$$

where α_g is the thermal expansion coefficient of the glass. This equation indicated qualitatively that tensile strain effectively shifts the temperature of the glass closer to T_g by an amount ΔT. Yield is expected when $\Delta T = T_g - T$.

Litt et al.[8,9] later pointed out that α_g is not a good approximation for the thermal expansion coefficient of the free volume in the glass, and proposed that it be replaced in Eq. (7) by $(\alpha_g - \alpha_c)$, where α_c is the thermal expansion coefficient of the completely crystalline state. Litt's modification does result in a more accurate description of yield behavior, but Eq. (7) cannot account for the dependence of the yield strain on strain rate or free volume, as will be shown. The existing free volume treatments give only a semi-quantitative description of the yield behavior of glassy polymers.

2.2 Kinetic Energy

A conceptual difficulty also arises with the free-volume theory. Though it is reasonable that a hole must exist in order for a segment to jump, the segment must possess sufficient kinetic energy to overcome the potential barrier opposing the transition. The free-volume theory alone does not take this energy effect into account.

Previously, Eyring,[22] and later Weymann,[23] treated this problem as applied to melt viscosity. They assumed the probability of a segment transition to be given by the product of two independent probabilities; the probability that the segment possesses sufficient kinetic energy, P_E, and the probability that sufficient local free volume exists, P_V. Their treatments, however, erred in the calculation of P_V, and the resulting equation fails to describe the temperature dependence of the viscosity of many polymer liquids.

It remained for Macedo and Litovitz[24] to combine the approaches of Eyring and Cohen and Turnbull to obtain an equation which describes the temperature and pressure dependence of the viscosity of polymer liquids. From their treatment

$$P_E \propto \exp(-E^*/RT) \tag{8}$$

and

$$P_V \propto \exp(-\gamma V^*/V_f) . \tag{9}$$

The quantity E* has the form of an Arhenius activation energy and represents the height of the potential barrier, including chain-restraining effects, between molecular segment equilibrium positions. R is the gas constant.

The parameter E* is of significance in the present work. The value of E* indicates the relative importance of free volume and energy effects, according to the theory, in the yield and relaxation processes. A high value of E* will be shown to mean that energy is most important, whereas a low value implies the opposite.

The probability of a molecular segment's making a transition is thus proportional to

$$P_T = P_E \cdot P_V \propto \exp(-E^*/RT) \cdot \exp(-\gamma V^*/V_f) . \tag{10}$$

Equation (10) is the basis for the yield and relaxation theory presented in the following pages. The equation was derived for, and has previously been applied to, the liquid state. It will be presumed in the following that Eq. (10) also is applicable to the glassy state. Such a presumption would appear unreasonable for a material which is crystalline as a solid, but seems plausible for an amorphous polymer, which undergoes no phase change during solidification. Provided that it can be extended to the glass, the above expression, derived for the liquid state, is entirely consistent with the model proposed in the introduction, as will be demonstrated.

2.3 Relaxation Times

In viscoelasticity theory, the Maxwell element is the model used to describe relaxation processes. The Maxwell element consists of a spring of constant K and a dash pot of constant η connected in series. The equation of motion of this element is

$$\dot{x} = \frac{\dot{F}}{K} + \frac{F}{\eta} \tag{11}$$

where x is the extension of the element, and F is the applied force.

In terms of material parameters, Eq. (11) becomes[25]

$$\dot{\sigma}(t) + \frac{\sigma}{\tau} = \dot{\varepsilon}E_o \tag{12}$$

where $\sigma(t)$ is stress, $\varepsilon(t)$ is strain, E_o is tensile modulus, and η is viscosity.

The relaxation time, τ, of the element is given by $\tau = \eta/E_o$. The relaxation time is a measure of the speed with which an applied stress relaxes. To see this, we solve Eq. (12) subject to the constraints of a stress-relaxation experiment. These constraints are that $\dot{\varepsilon} = 0$ and $\sigma(0) = \sigma_o = \varepsilon_o E_o$. We obtain

$$\sigma(t) = \sigma_o \exp(-t/\tau). \tag{13}$$

Equation (13) describes the variation of stress with time during a stress-relaxation experiment. To obtain the expression defining the modulus during such a test, both sides of Eq. (13) are divided by ε_o, the initial applied strain. We obtain

$$E(t) = E_o \exp(-t/\tau) \tag{14}$$

where $E_o = \sigma_o/\varepsilon_o$.

In order to describe the relaxation behavior of real polymers adequately, it is necessary to assume the material to be made up of an infinite number of Maxwell elements, with a distribution of relaxation times. Equation (14) becomes

$$E(t) = \int_{-\infty}^{\infty} H(\tau) \exp(-t/\tau)\, d\ln\tau \tag{15}$$

where $H(\tau)$ is the relaxation-time distribution function.[26]

It is clear from Eq. (15) that relaxation processes are determined by τ and $H(\tau)$. According to the WLF assumption,[17] for $T > T_g$, the effect of a change in temperature is to shift the relaxation spectrum, shape unchanged, to higher or lower values of τ. An analogous assumption will be made for the glassy state in the present work; it will be assumed that a change in free volume also shifts the spectrum without changing its shape. Thus, to show the relationship between yield and relaxation using the free-volume theory, it is necessary to obtain expressions for τ and yield strain from the theory.

The relaxation times of a polymer can be assumed inversely proportional to the probability of a molecular transition.[24,27] Hence,

$$\tau \propto P_T^{-1} \propto \exp(E^*/RT) \exp(\gamma V^*/V_f) . \tag{16}$$

wn that relaxation times decrease with decreas-
ndicates that the proportionality constant
t be positive. Equation (16) shows that as
pecimen, and thus as free volume increases
decreases, as it should in order to agree with
ation proposed in the introduction. Equation (16)
ich relates relaxation to the free-volume theory.
e used to derive an expression for the shift
factor is defined in terms of relaxation

$$a_T = \frac{\tau_p(T)}{\tau_p(T_o)} \qquad (17)$$

elaxation time at temperature T, and
tion time at the reference temperature.
, one obtains

$$\frac{\gamma V^*[V_f(T_o) - V_f(T)]}{V_f(T_o)V_f(T)} + \frac{E^*(T_o - T)}{2.303RT_oT} \qquad (18)$$

ndence, according to the theory, of the shift
d free volume. For temperatures greater than
uilibrium and total free volume, V_f, is equal
me, v_f. In this case, taking T_o greater
r is given by

$$= \frac{-C_1(T - T_o)}{C_2 + T - T_o} - \frac{E^*(T - T_o)}{2.303RT_oT} \qquad (19)$$

$\alpha_f)$, $C_2 = T_o - T_2$, and $V_f(T) = \Delta\alpha_f(T - T_2)$.
ld describe the behavior of the shift factor
er than T_g. Equation (16) can be written for
s

$$\exp(E^*/RT)\exp\left[\frac{2.303C_1C_2}{T - T_o + C_2}\right]. \qquad (20)$$

below the glass transition the polymer is not in
and total free volume is not equal to equilibrium
ses both an equilibrium and nonequilibrium
nequilibrium free volume w_f, which determines
racter of the glassy state through its dependence
ry of the polymer.

[,19,28] that when an amorphous polymer is rapidly
ature above its glass transition to a temperature
he polymer continues to decrease with time even
ium has been established. This "isothermal
y be a result of nonequilibrium free volume
lymer. Nonequilibrium free volume can then be
t of the total free volume which is not fixed
ibrium free volume is determined completely by
hermal history of the polymer cannot alter its
and, w_f is determined only by thermal history,
ure-dependent range, may assume any value.
lower than the glass transition, then,
t be rewritten to include w_f. These expressions

$$03C_1C_2[C_2\Delta\alpha_f - v_f(T) - w_f(T)] \over C_2[v_f(T) - w_f(T)]} + \frac{E^*(T_o - T)}{2.303RT_oT} \qquad (21)$$

$$\exp(E^*/RT)\exp\left[\frac{2.303C_1C_2\Delta\alpha_f}{v_f(T) + w_f(T)}\right]. \qquad (22)$$

e the dependence of relaxation times and the rature and free volume in the glassy state. plicated, a convenience in notation introduced . The effective temperature, T_e, is defined as

$$= T_2 + w_f/\Delta\alpha_f \qquad \text{for } T \leq T_2$$

$$(23)$$

$$= T + w_f/\Delta\alpha_f \qquad \text{for } T \geq T_2.$$

, one can show that the effective temperature e nonequilibrium glass at temperature T has cal to those of the hypothetical-equilibrium (T). Recasting Eqs. (21) and (22) in terms ature gives

$$T = \frac{-C_1(T_e - T_o)}{C_2 + T_e - T_o} - \frac{E^*(T - T_o)}{2.303RT_oT} \qquad (24)$$

$$\exp(E^*/RT)\exp\left[\frac{2.303C_1C_2}{T_e - T_o + C_2}\right]. \qquad (25)$$

s conceptually useful in allowing Eqs. (19) and e liquid state, to be used for the glass by n the volume factors of those equations.

2.4 Yield Strain

f the occurrence of a molecular transition is erse of τ as defined by Eq. (25). According pplied to the glass increases free volume. volume is fixed by temperature, this strain-rease amounts to an increase in nonequilibrium g the case, Eq. (23) shows that applied strain temperature of the glass. The amount of on how much of the strain-induced volume cor-, i.e., the value of β in Eq. (6). In the taken as unity. This value implies that all orresponds to free volume.

perature of the glass can then be thought of as arts: T_e', that part determined by temperature en by Eq. (23), and ΔT_e, the strain-dependent

$$T_e = \frac{\Delta V}{\rho \Delta \alpha_f} = \frac{(1 + \varepsilon)^{1-2\mu} - 1}{\rho \Delta \alpha_f}. \qquad (26)$$

ws that as T_e increases, τ decreases causing $_T$ reaches some critical value, $P_{T_{cr}}$, dependent

n rate, and thermal history, relaxational
fast enough to cause the material to relax
f the experiment and yield to initiate. Put
aches a critical value, yielding should begin.
strain as a function of temperature thus can
g

$$E^*/RT)\exp\left[\frac{-2.303C_1C_2}{T'_e+\Delta T_e-T_o+C_2}\right]\propto P_{T_{cr}} \qquad (27)$$

ording to Eq. (26). To obtain an expression
alue of $P_{T_{cr}}$ must be found.

some temperature at which, in the absence of
ume, the transitional probability is equal to
ure, an infinitesimal applied strain would

In order for this to happen, the polymer must
tate. Therefore the temperature at which the
t be near T_g. That temperature will be denoted

to T_g, nonequilibrium free volume must be nearly
$^*_g$. Under these conditions, we may write

$$\propto \exp(-E^*/RT^*_g)\exp\left[\frac{-2.303C_1C_2}{T^*_g-T_o+C_2}\right]. \qquad (28)$$

n Eqs. (27) and (28), and substituting ΔT_e from

for ε_y, the strain at yield initiation,is

$$C_2-T'_e + \Bigg[\bigg[\frac{1}{C_2-T_o+T^*_g} + \frac{E^*(T-T^*_g)}{2.303C_1C_2RT^*_gT}\bigg]^{-1}\Bigg]+1. \qquad (29)$$

ribes the variation of yield strain with tem-
temperature, and may be used to predict the
ain upon any variable which can be related to
re.

ain rate on yield strain is introduced through
T^*_g, which will be taken to change with rate in
$_g$. It has been shown[29,30] that time-temperature
able to constant strain-rate experiments with
cates the strain rate at temperature T, for
response is identical to that at $\dot{\varepsilon}_o$ and T_o. We

$$\frac{T^*_g}{\text{og } \dot{\varepsilon}}\Bigg]_{T,P} = -\Bigg[\frac{\partial\ T^*_g}{\partial \log a_T}\Bigg]_{\dot{\varepsilon},P} . \qquad (30)$$

ing $\tau_p(T)$ from the inverse of Eq. (28), we have

$$\frac{(T^*_g - T_o)}{+\ T^*_g - T_o} - \frac{E^*(T^*_g - T_o)}{2.303RT^*_gT_o}. \qquad (31)$$

, one then obtains

$$\frac{C_1C_2}{{}^*_g(\dot{\varepsilon})-T_o]\ [C_2+T^*_g(\dot{\varepsilon}_o)-T_o]} + \frac{E^*}{2.303RT^*_g(\dot{\varepsilon})T^*_g(\dot{\varepsilon}_o)}\Bigg]^{-1}. \qquad (32)$$

calculate the strain-rate dependence of

e dependence of ε_y.

2.5 Relaxation Rate

defined as the negative of the slope of the

rve for a stress-relaxation experiment. From

$$e = - \left[\frac{\partial}{\partial \log t} [\log \int_{-\infty}^{\infty} H(\tau) \exp(-t/\tau) \, d\ln\tau] \right]_{T,\varepsilon} \qquad (33)$$

ate with free volume and temperature can be

33) and (25). The effect of such a change on

(25). Then, from the change in τ, one can

n rate using Eq. (33).

3. DETERMINATION OF INITIAL YIELD POINT

3.1 Volume-Elongation Measurements

An experiment which should determine the initial yield point is the measurement of the volume change undergone by a polymer glass during extension. When a small tensile strain is imposed upon a material, the volume increase which accompanies the strain is described by Eq. (4)

$$\frac{\Delta V}{\varepsilon} = V_o(1-2\mu) . \tag{4}$$

Poisson's ratio, and thus the ratio $\Delta V/\varepsilon$, should be constant within the Hookean region. As the glass is strained, the mobility of the chains should increase until it is such that the relaxation rate approaches equivalence with the strain rate, and the glass yields. Strained past initial yield, the polymer should behave more like a liquid and less like a glass because of increased chain mobility. A corresponding increase in μ will accompany the glass-liquid transition as well until, at necking, $\mu = 0.5$ and the polymer draws as a viscous liquid. Therefore, in monitoring volume versus elongation, one should observe a constant slope up to yield initiation, then a decrease in the slope to zero as draw is realized.

An instrument with which to make such measurements, the tensile-extension dilatometer, was designed and constructed. Details of the design may be found in the Appendix. Measurements were made on PMMA from -20°C to 100°C in increments of 20°C; the experimental procedure is also described in the Appendix.* Because of the method used for the measurement of volume change, an irregular line for ΔV versus elongation was obtained, a smoothed version of that curve for T = 60°C is shown in Figure 8. Curves for the other test temperatures are shown in the Appendix. These figures show that, as predicted, the slope of the volume-elongation plot is constant to ε_A, then decreases to zero at ε_B. Therefore, ε_A must correspond to yield initiation.

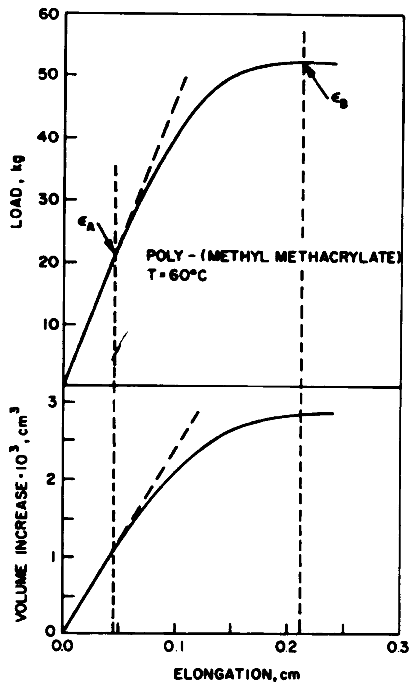

Figure 8--Tensile-extension dilatometer data for PMMA for T = 60°C.

It should be noted that the behavior displayed in Figure 8 could arise from either bulk yield on a macroscopic scale, or microscopic yield of small regions. Whichever is the

---

*All testing described in this report was carried out on an MTS closed-loop, electro-hydraulic testing machine. The MTS was equipped with an environmental chamber which held temperature constant to within 0.25°C.

case, on a molecular scale large deformation of molecular segments is occurring, and yield is taking place.

The figure also shows that the point at which the slope of the load-elongation curve begins to decrease, commonly termed the "proportional limit," occurs at approximately the same elongation as ε_A. Similar results were obtained at each temperature at which a volume-elongation yield point was observed, as shown in Table 1.

TABLE 1

YIELD ELONGATION VERSUS TEMPERATURE
OBTAINED FROM VOLUME MEASUREMENTS

$T, ^\circ C$	Yield Elong. (vol), cm	Prop. Lim. Elong., cm
-20	pre-yield fracture	pre-yield fracture
0	0.094	0.090
20	0.074	0.078
40	0.060	0.058
60	0.047	0.047
80	no observable Hookean region	
100	no observable Hookean region	

Analogous results were obtained by the author for polycarbonate, and Whitney and Andrews[11] have reported data for several glasses loaded in compression which bear out these results.

3.2 Fractional Hysteresis-Elongation Measurements

A second experiment which should determine the point of yield initiation is the measurement of the fractional hysteresis of a glass as a function of maximum applied elongation for single tensile load-unload cycles run at constant frequency. Linear viscoelasticity

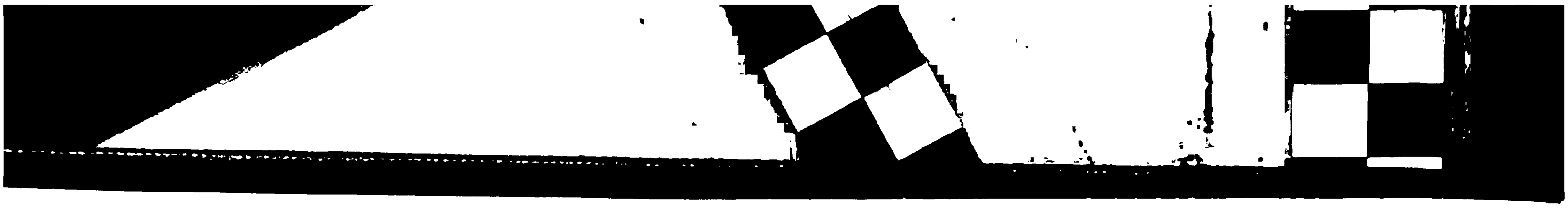

theory predicts that at a given frequency of test, fractional hysteresis should be independent of applied strain. Fractional hysteresis is defined as the difference between energy applied to the specimen during loading and energy returned by the specimen during unloading divided by the energy applied. For a single Maxwell element model, solution of Eq. (12) subject to the initial condition $\sigma(0) = 0$ gives

$$\sigma(t) = \tau\dot{\varepsilon}E_o(1 - e^{-t/\tau}). \qquad (34)$$

A constant-frequency, single-cycle load-elongation experiment is described by the plot of applied strain versus time shown in Figure 9. From Eq. (34) and Figure 9, the stress exerted on a specimen during

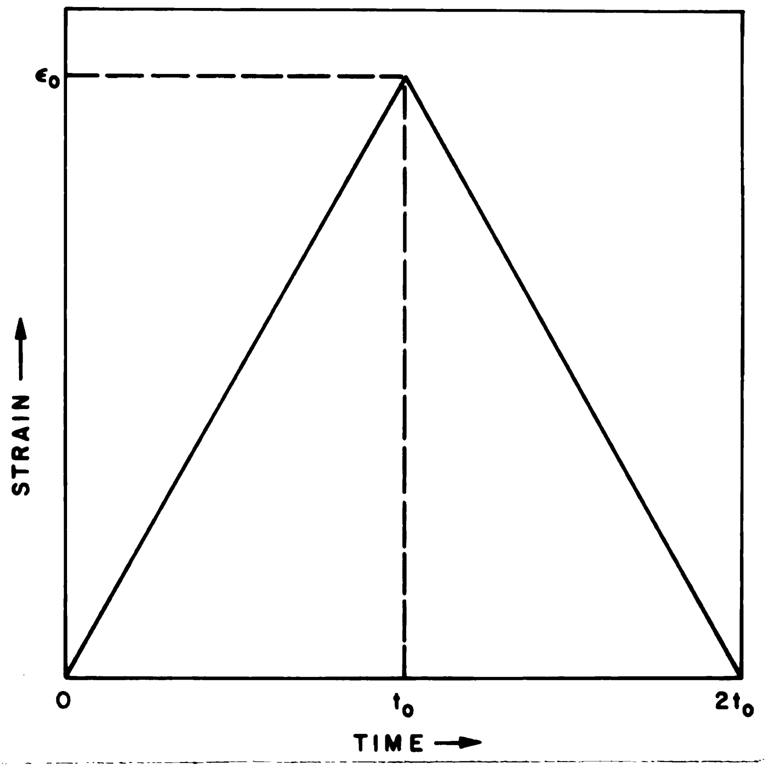

Figure 9--Strain-time diagram for constant-frequency, single-cycle load-elongation experiment.

such an experiment can be calculated. For $0 \leq t \leq t_o$, that stress is found to be

$$\sigma(t) = \tau E_o \frac{\varepsilon_o}{t_o} (1 - e^{-t/\tau}). \tag{35}$$

By application of the Boltzmann superposition principle,[31] the stress in the region $t_o \leq t \leq 2t_o$ is obtained

$$\sigma(t) = \tau E_o \frac{\varepsilon_o}{t_o} (1 - e^{-t/\tau}) - 2\tau E_o \frac{\varepsilon_o}{t_o} (1 - e^{-(t-t_o)/\tau}). \tag{36}$$

Integration of Eqs. (35) and (36) in terms of strain, followed by division of the sum of those integrals by the integral of Eq. (35) gives the fractional hysteresis, W.

$$W = 1 + \frac{t_o/\tau + (e^{-t_o/\tau} - 1)(2 - e^{-t_o/\tau})}{t_o/\tau + e^{-t_o/\tau} - 1}. \tag{37}$$

The above equation shows that for a single Maxwell element, W is independent of ε_o, and depends only upon test frequency t, and τ, the relaxation time of the element. Chang[26] has shown that the same result holds for a model consisting of an infinite number of elements and a distribution of relaxation times.

It would seem that prior to yield, linear viscoelasticity should hold, since in this region the relaxation times of the glass are such that the rate of relaxation is much lower than the loading rate. In such a situation the material should behave in nearly a Hookean manner, and fractional hysteresis ought to be small and constant, or slightly increasing (as a result of strain-induced mobility) with ε_o. At the yield point, in accordance with the yield-relaxation relation proposed in the introduction, the relaxation rate has become equivalent to the strain rate, and the polymer chains are better able to respond to the stress during the time of the test. As a result of the enhanced relaxation, some permanent, nonelastic deformation, or flow, will occur, increasing the amount of energy lost in the deformation, and so increasing W. The energy loss should continue to increase with increasing strain past yield. When W is plotted versus ε_o, tests should show a constant or slightly increasing value of W up to yield, then W should continue to increase with ε_o past yield.

Tensile tests were run on specimens of PMMA with cross-sectional dimensions of 0.5 cm by 0.318 cm and with a distance of 5 cm between grips. The loading function was that of Figure 9 with $t_o = 10$ seconds and ε_o varying. Measurements were carried out at temperatures of 0°C, 20°C, 40°C, and 60°C. Specimens were annealed at 130°C for one hour, then quenched between steel plates at the test temperature. Testing was begun 30 minutes after quench. Figure 10 shows the results of the test at T = 20°C.

The zero-slope line represents the average value of the first seven points. Zero slope was chosen for convenience, but according to the theory it may be slightly positive. The line of nonzero slope is a least-mean-squares fit to the remaining points. The load-elongation curve shown in the figure corresponds to a maximum elongation of 0.1 cm which represents a median value of strains applied to the specimens.

The figure shows that the point at which linear viscoelasticity begins to fail is near the proportional limit of the load-elongation

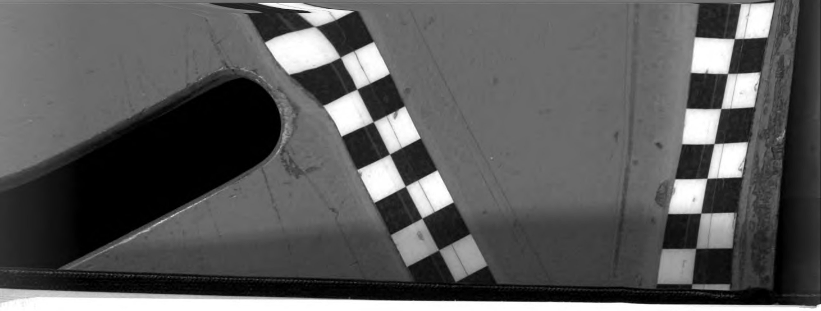

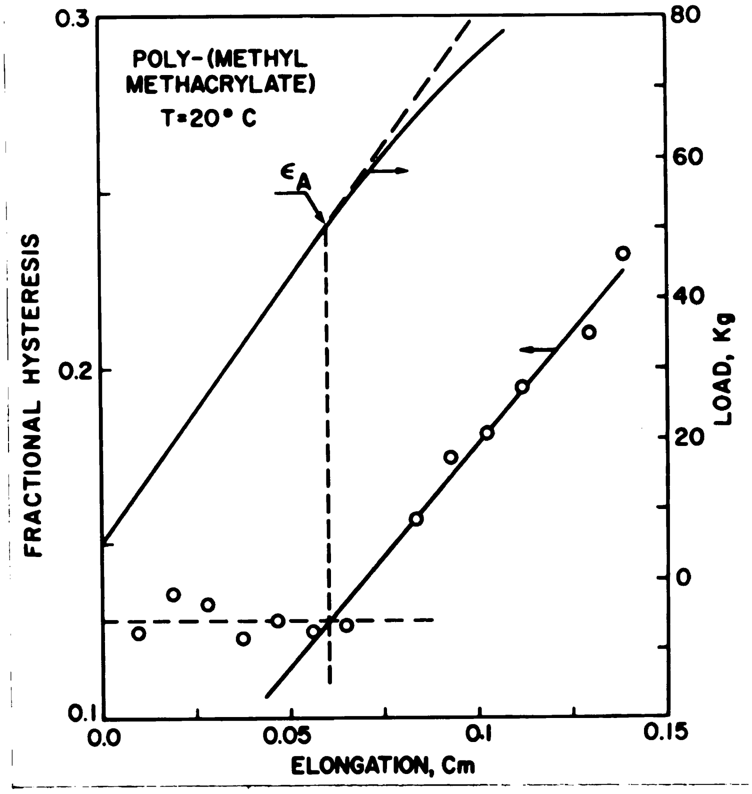

Figure 10--Fractional hysteresis data for PMMA for T = 20°C.

curve. Such correspondence held at each test temperature, as is shown in Table 2.

TABLE 2

YIELD ELONGATION VERSUS TEMPERATURE OBTAINED FROM HYSTERESIS MEASUREMENTS

T,°C	Yield Elong.(hys),cm	Prop. Lim. Elong.,cm
0	0.070	0.068
20	0.060	0.060
40	0.045	0.048
60	0.040	0.043

Experimental data for the other test temperatures are given in the Appendix.

Results of two independent tests, carried out over a wide temperature range, show that the initial yield point occurs at about the same value of strain as the proportional limit of the tensile load-elongation curve. This suggests that the proportional limit of the load-elongation curve should be taken to indicate yield initiation, a finding which will come as no surprise to metallurgists, who have accepted the fact for metals for many years. It is likely to be considered unusual for polymers, however, where the maximum of the curve traditionally has been taken to denote yield. Probably the proportional limit would have been recognized as the yield point earlier if more work had been done on polymer glasses, rather than on melts and solutions.

It should be noted that one cannot state unequivocally that yield begins exactly at the proportional limit. The proportional limit itself is not an exact point, but varies slightly according to the person choosing it. If the yield process is relaxational in nature, then, just as the glass transition takes place over a range of temperatures, yield will occur over a range of strain. This range, though only few tenths of one percent strain, limits the precision with which the yield point can be determined.

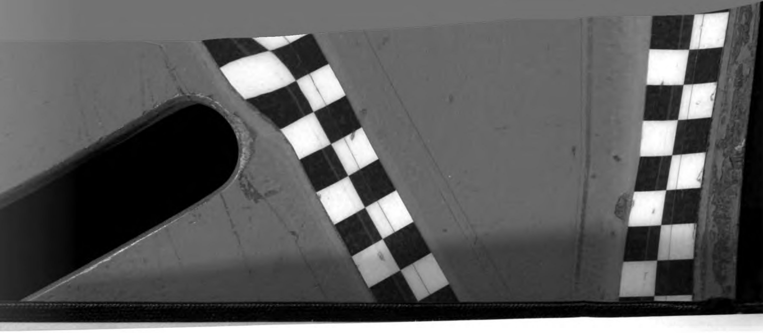

4. YIELD AND RELAXATION MEASUREMENTS

4.1 Yield Strain

Having determined that the proportional limit of the load-elongation curve is indicative of initial yield, the investigation of glassy yield was begun. The variation of initial yield strain with temperature, strain rate, and free volume was studied. The effect of free volume was assessed by testing during isothermal volume contraction.

Tension tests were run on PMMA from -10°C to 100°C, over a range of strain rates from 0.015%/second to 120%/second. The geometry of the test specimens is shown in Figure 11. The shape eliminates the possibility of grip slippage and compressive end effects associated with the standard tensile specimen, as well as being quickly and easily mounted in the environmental chamber at all temperatures.[13] The effective length of the specimens was found to be 6.6 cm, determined by comparing the modulus of the tensile test specimens with the modulus of flexure specimens tested under identical thermal conditions. For the yield point tests, each specimen was annealed at 130°C for one hour, quenched between steel plates to the test temperature, and held for 30 minutes prior to test. The proportional limit of each load-elongation curve was found. The results are plotted in Figure 12 as yield strain versus temperature, where the estimated error in choosing the proportional limit is indicated by a bar. No data points are shown for

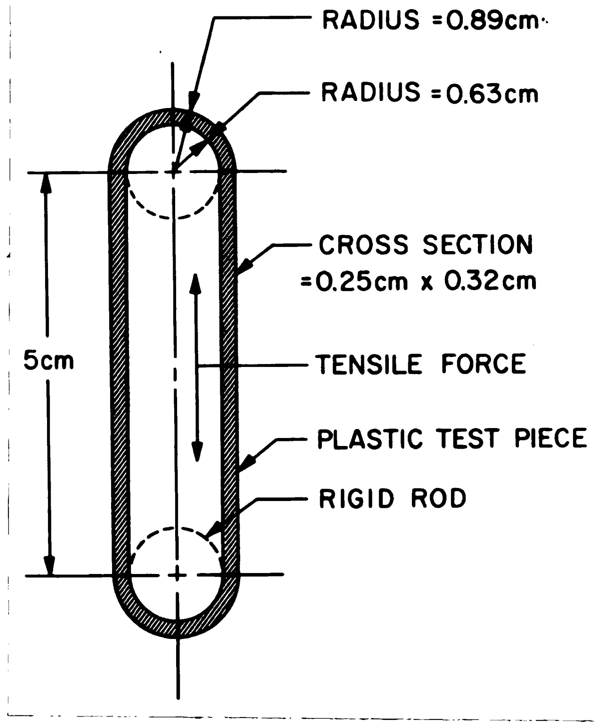
RADIUS =0.89cm
RADIUS =0.63cm
CROSS SECTION =0.25cm x 0.32cm
TENSILE FORCE
PLASTIC TEST PIECE
RIGID ROD
5cm

Figure 11-Tensile-test specimen configuration.

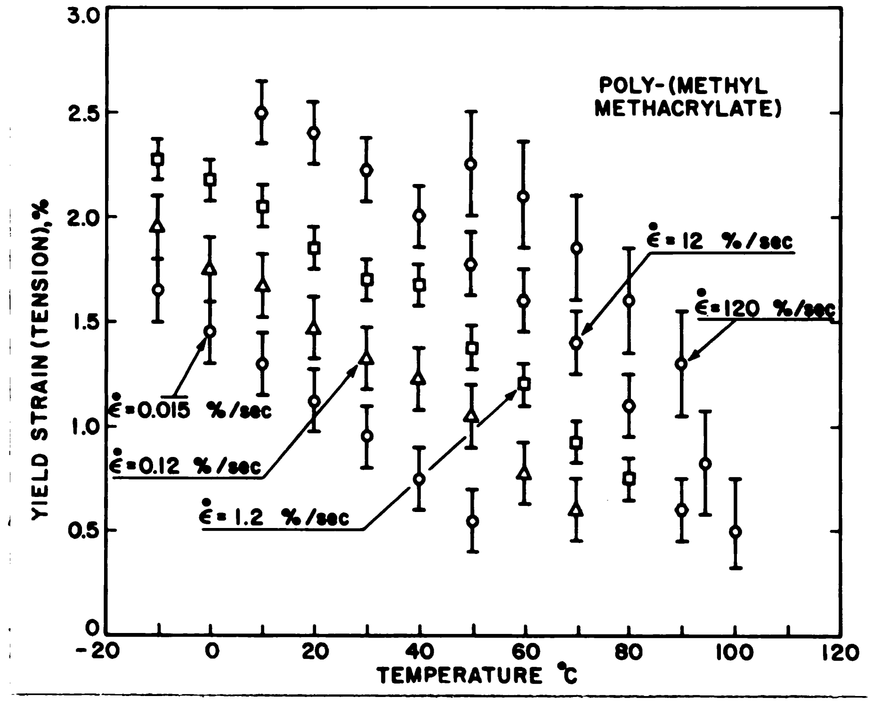

Figure 12--Yield strain of PMMA as a function of temperature and strain rate.

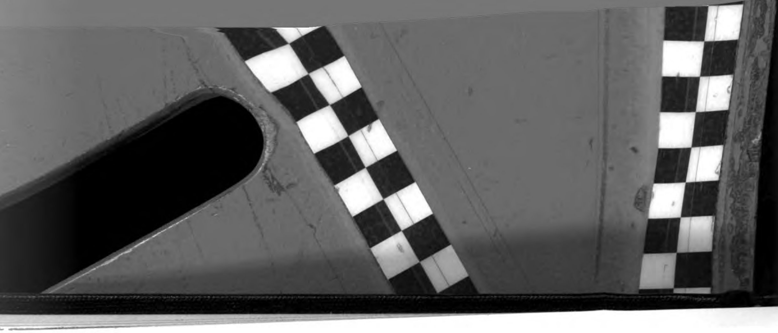

yield strains less than 0.5% or greater than about 2.5%. When the yield strain was small, no Hookean region was observed, and when the yield strain was high, specimen fracture occurred prior to yield.

To investigate the effect of changes in free volume in the absence of temperature or rate changes, yield was measured during isothermal volume contraction. A series of tests was carried out on PMMA from 40°C to 90°C. Specimens were annealed at 130°C for one hour, then quenched between steel plates to test temperature. Testing was done at increasing times after quench in flexure, with specimens 7.5 cm long, 2.5 cm wide, and 0.318 cm thick. Test pieces were supported on two 0.318 cm diameter rollers spaced five cm apart, with the load applied by a third similar roller midway between the first two. Since the flexure test is inherently nonlinear, even for a Hookean material, it was necessary to apply a correction[32] to determine the location of the proportional limit. Yield was taken as the point of departure of the calculated Hookean curve from the experimental curve, as shown schematically in Figure 13.

The results of the tests are shown in Figure 14, where yield strain is plotted versus the logarithm of time after quench, log t_q. The solid lines are least-mean-squares fits to the data. It should be noted that neither of the currently accepted and commonly applied theories of yield, the Von Mises deviatoric-strain-energy criterion, nor the Tresca maximum-shear-stress theory, can account for the dependence of the yield point upon free volume. It is necessary that any theory proposed to describe yield of polymeric glasses account not only for the temperature and rate dependence of yield, but also for free volume-yield relationship.

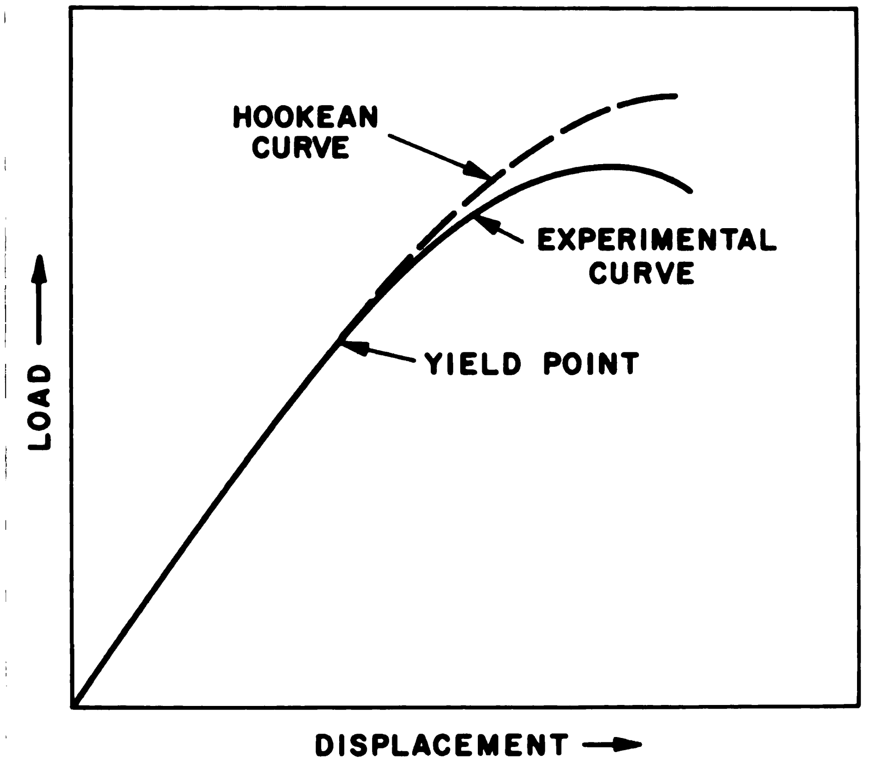
HOOKEAN CURVE
EXPERIMENTAL CURVE
YIELD POINT
LOAD
DISPLACEMENT

Figure 13--Schematic drawing showing method of yield point determination for a flexural test.

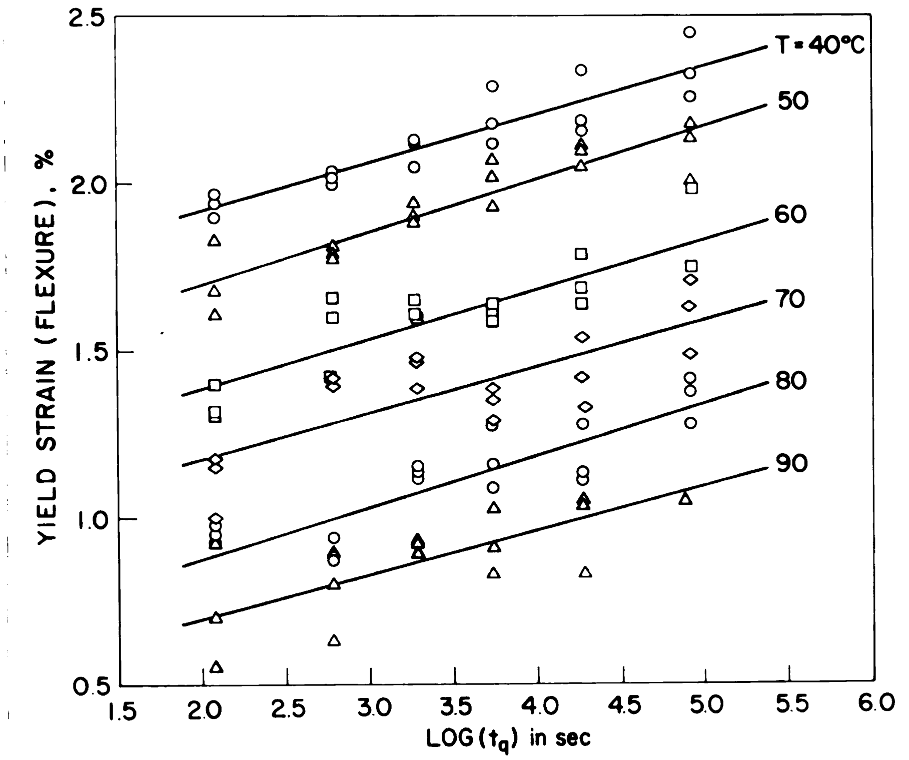

Figure 14--Yield strain of PMMA as a function of time after quench.

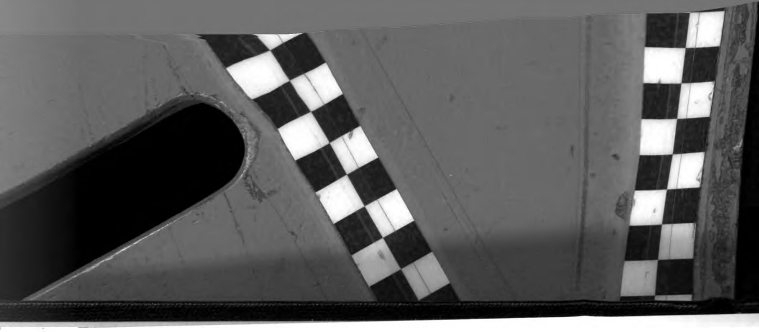

4.2 Relaxation Rate

In this work, the relaxation behavior of PMMA glass will be taken to be indicated by the relaxation rate as measured during a stress-relaxation experiment. The variation of relaxation rate with changes in temperature, maximum applied elongation, and time after quench during isothermal volume contraction will be considered. The effect of temperature upon relaxation rate is already well documented[13] (Figure 15). For the present work, the two other dependencies were investigated.

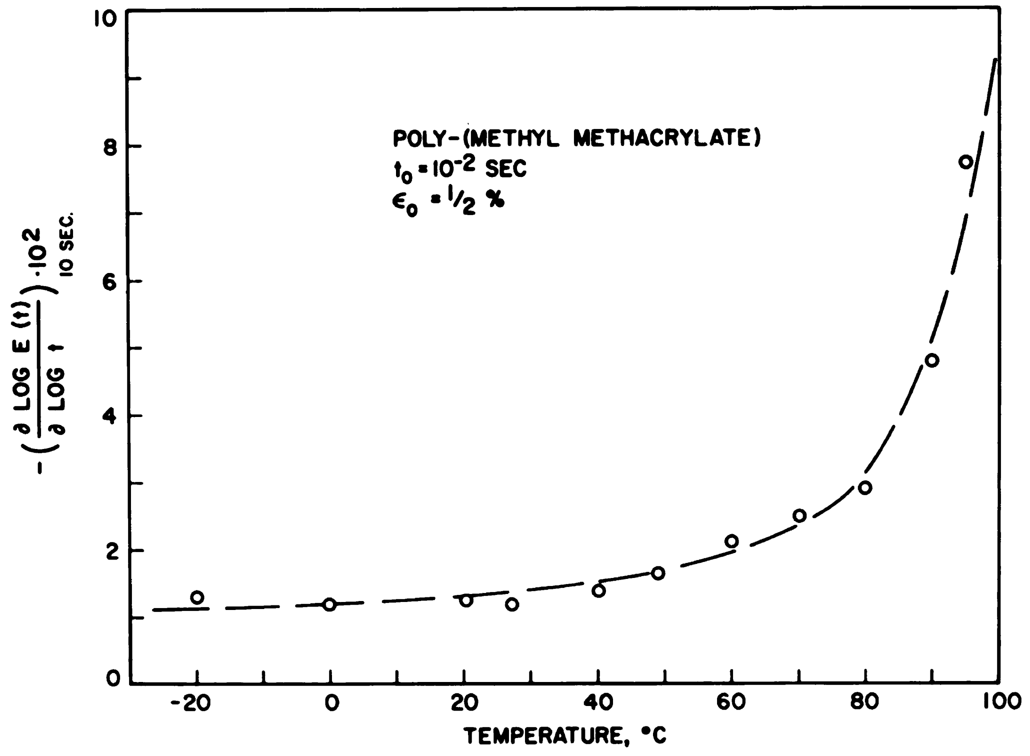

Figure 15--Ten-second relaxation rate of PMMA as a function of temperature.

Measurement of the ten-second relaxation rate as a function of maximum applied elongation was effected at 60°C and 80°C using the ring-shaped specimens previously described. The specimens were used

in the as-received condition. A given elongation was applied to the test pieces in 10^{-2} seconds, and the load required to maintain that elongation was monitored as a function of time thereafter. From the data, the ten-second relaxation rate, $-(\partial \log E(T)/\partial \log t)_{t\,=\,10\text{ sec}}$ was calculated. Testing was done for increasing values of elongation up to specimen fracture. Figure 16 shows the results.

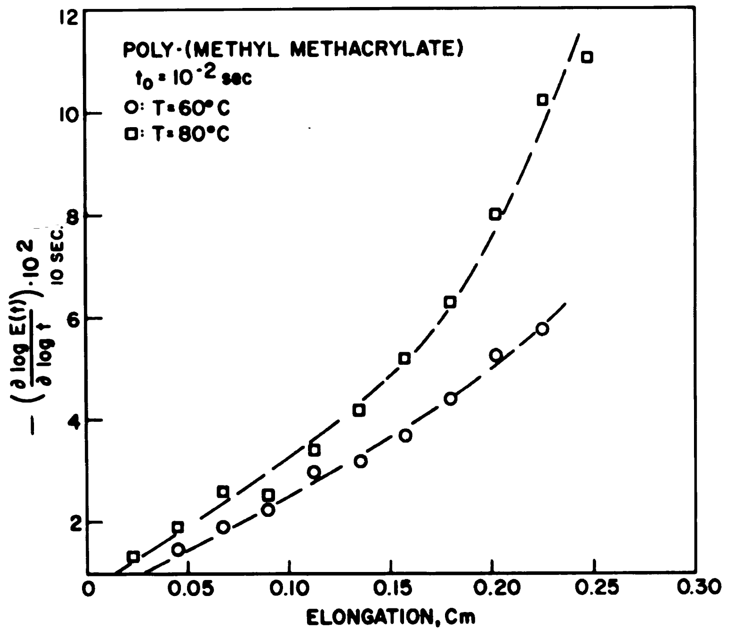

Figure 16--Ten-second relaxation rate of PMMA as a function of applied elongation.

Measurement of relaxation rate as a function of time after quench was carried out at 30°C and 50°C. Specimens were given the standard thermal pre-treatment. Tests were run in flexure at various times after quench. A midpoint surface strain of 0.1% was applied in 10^{-2} seconds, and the ten-second relaxation rate was obtained. Figures 17 and 18 show the results.

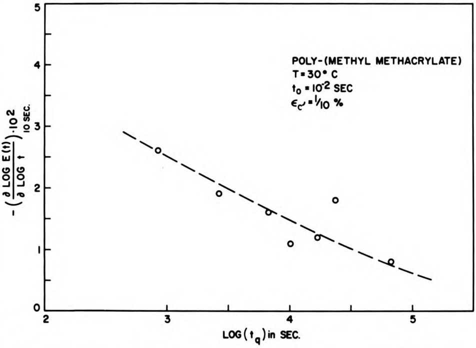

Figure 17--Ten-second relaxation rate of PMMA as a function of time after quench for T = 30°C.

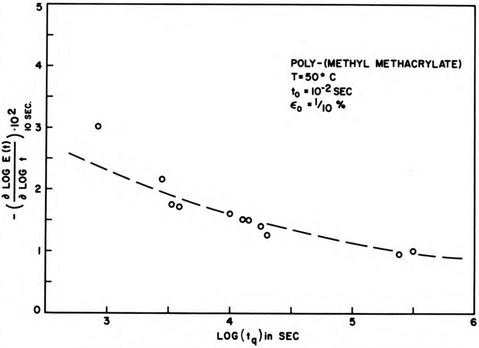

Figure 18--Ten-second relaxation rate of PMMA as a function of time after quench for T = 50°C.

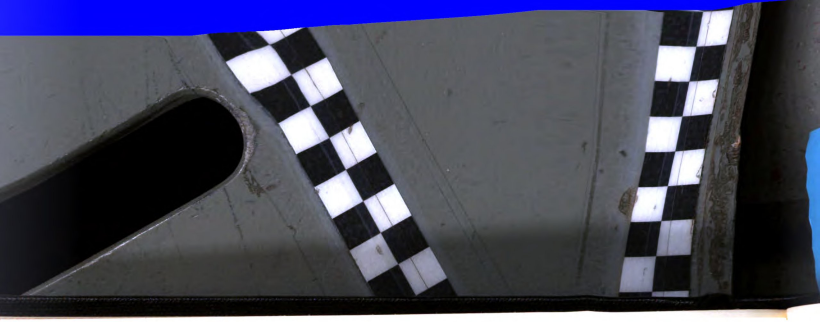

5. COMPARISON OF THEORY AND EXPERIMENT

5.1 Yield Strain

To compare theoretical with experimental results for yield strain and relaxation rate, it is necessary to evaluate the material parameters μ, E^*, C_1, C_2, and $\Delta\alpha_f$. Poisson's ratio, μ, was determined for the present work from the volume-elongation measurements described previously. The initial slope of the volume-elongation plot, $\Delta V/\Delta \ell$ (volume change/length change), was measured, and Eq. (4) in the form

$$\mu = 0.5[1 - \Delta V/(A\Delta \ell)] \qquad (37)$$

where A is the cross-sectional area of the narrowest portion of the specimen used to calculate μ.

Results of these calculations are shown in Figure 19, a plot of μ versus temperature. Each data point is the average of two or more measurements. It is seen that Poisson's ratio is temperature dependent. Other workers have found values of μ for PMMA from 0.34 to 0.4 at room temperature.[11,33,34] However, no other results have been published in which μ is obtained from volume measurements made over a wide temperature range. Such an increase of Poisson's ratio with temperature is not surprising since the glass does tend to become more like a liquid as the glass transition temperature is approached. Several tests were also run at a rate of extension ten times faster than the standard

rate (0.001 cm/sec) and to within experimental error, no rate effect was noted.

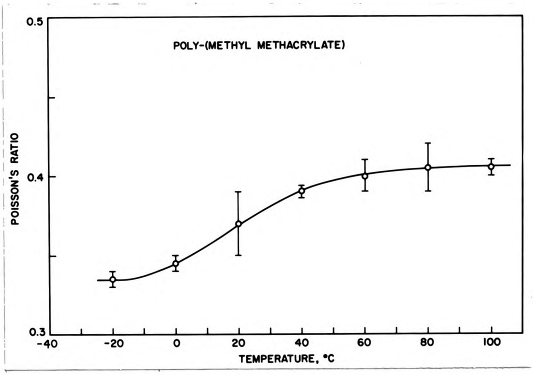

Figure 19--Poisson's ratio of PMMA as a function of temperature.

The values of μ used for each temperature are described by the solid curve of the figure; these are listed in Table 3, along with values of the specific volume ($1/\rho$) from Figure 7.

The constants E^*, C_1, C_2, and $\Delta\alpha_f$ are all interrelated and may therefore be considered as a single parameter. In other words, if the value of E^* is determined, C_1, C_2, and $\Delta\alpha_f$ are specified. At $T > T_g$, Eq. (19) should hold for log a_T as a function of temperature. For a given value of E^*, using log a_T data for $T > T_g$ (Figure 20), the factor $(T - T_o)/[\log a_T + E^*(T - T_o)/(2.303RTT_o)]$ may be plotted versus $(T - T_o)$. The slope of the resultant straight line is $-1/C_1$, and its intercept is $-C_2/C_1$. In this manner, for any value of E^*, the corresponding values of C_1 and C_2 can be found.

TABLE 3

POISSON'S RATIO AND SPECIFIC VOLUME FOR PMMA

T, ^{o}C	μ	$1/\rho$, cm^3/g
-20	0.333	0.8540
-10	0.337	0.8555
0	0.344	0.8563
10	0.353	0.8568
20	0.363	0.8585
30	0.376	0.8603
40	0.390	0.8622
50	0.398	0.8641
60	0.403	0.8649
70	0.407	0.8668
80	0.411	0.8689
90	0.413	0.8721
100	0.414	0.8746

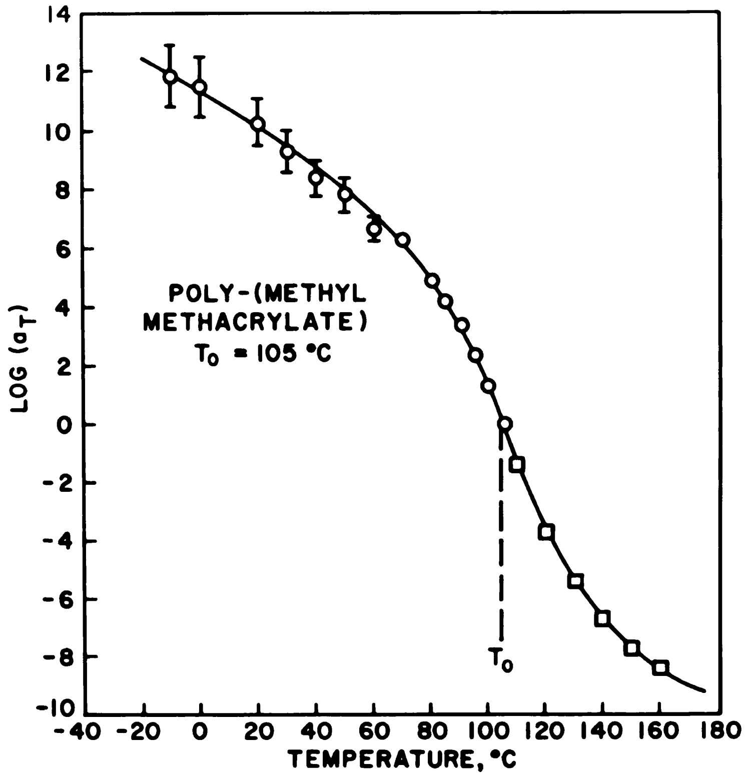

Figure 20--Log a_T of PMMA as a function of temperature for $t_q = 10^4$ seconds.

With E* and the calculated values for C_1 and C_2, data for log a_T in the glassy state may be used to obtain the effective temperature, $T_e(T)$ from Eq. (24). The quantity $V_t - V_\infty$ is known from isothermal volume contraction data. V_t is the polymer specific volume at time t after quench from above T_g, and V_∞ is the volume corresponding to the extrapolation of the liquid line in Figure 7. It can be shown from Eq. (23) that for any temperature

$$T_e(T) = T + \frac{V_t - V_\infty}{\Delta\alpha_f} . \qquad (38)$$

From Eq. (38) and the isothermal volume contraction data, $\Delta\alpha_f$ is obtained. Time after quench must be the same for the log a_T data and for V_t, in this case 10^4 seconds. Figures 20 and 21 show

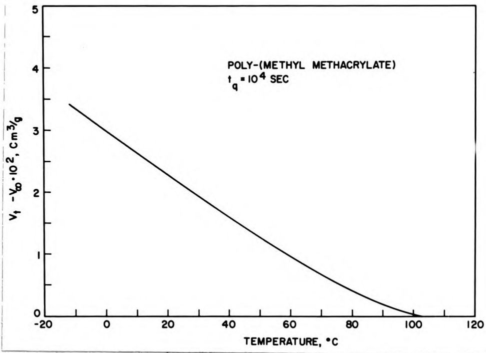

Figure 21--$V_t - V_\infty$ of PMMA as a function of temperature for $t_q = 10^4$ seconds.

respectively the log a_T data and the isothermal volume contraction data used in the present work.[13] Although in the free-volume theory $\Delta\alpha_f$ is assumed constant, the calculated values vary slightly with temperature (about 10% from -20°C to 100°C). An average value is chosen.

By the above method, a consistent set of values for E*, C_1, C_2, and $\Delta\alpha_f$ may be found. Table 4 lists these values for several values of E*. A value of E* of 35 Kcal/mole corresponds to an iso-free volume state, since for that case, $\Delta\alpha_f = \alpha'_\ell - \alpha'_g$. This indicates that $\alpha'_{g(t\to\infty)} = \alpha'_g$, so nonequilibrium free volume would be constant with temperature. The value of 35 Kcal/mole therefore represents the upper limit of E* consistent with the present theory. In this limit free volume could have no relation to changes in yield or relaxation behavior with temperature, and such phenomena would have to be attributed solely to energy effects.

TABLE 4

CALCULATED MATERIAL CONSTANTS FOR PMMA FOR GIVEN VALUES OF E*.

E*, Kcal/mole	C_1, °C	C_2	$\Delta\alpha_f$, g/cm^3-°C$\cdot 10^4$
0	16.1	49.8	3.45
5	15.1	47.4	3.37
10	14.0	44.9	3.29
15	13.0	42.3	3.22
20	12.1	39.8	3.14
25	11.1	37.1	3.06
30	10.2	34.5	2.98
35	9.3	31.8	2.90

Though C_1, C_2, and $\Delta\alpha_f$ may be calculated, given E*, the value of E* itself must be known. The problem of determining this experimentally proved to be a difficult one. The quantity $(\partial \log a_T/\partial V_f)_T$ can be

evaluated experimentally from the shift in relaxation modulus occurring during isothermal volume contraction.[19,35,36] A theoretical expression for that quantity is obtained by differentiating Eq. (24) with respect to V_f, which gives

$$(\partial \log a_T/\partial V_f)_T = \frac{-C_1C_2}{(C_2+T_e-T_o)^2}\cdot\frac{1}{\Delta\alpha_f}. \quad (39)$$

Inasmuch as C_1, C_2, $T_e(T)$, and $\Delta\alpha_f$ are dependent upon E*, a comparison of experimental results for $(\partial \log a_T/\partial V_f)_T$ with those results calculated for various assumed values of E* would seem to determine the quantity.

The experimental procedure followed in obtaining the dependence of the shift factor on free volume is described below. Flexural specimens were annealed at 130°C for one hour and quenched between steel plates to the test temperature, then stress-relaxation experiments were run at increasing times after quench. Testing was carried out from 50°C to 100°C. A maximum midpoint surface strain of 0.1% was applied in 10^{-2} seconds. Figure 22 shows a typical set of data. The resulting data were shifted in the usual manner and plotted as shown in Figure 23. The slope of the plot is $(\partial \log a_T/\partial V_f)_{70}$. This quantity is then divided by the factor $(\partial V_f/\partial \log t_q)_T$, obtained from isothermal volume-contraction data,[13] to give the experimental values for $(\partial \log a_T/\partial V_f)_T$. Table 5 lists the numbers used for $(\partial V_f/\partial \log t_q)_T$. Theoretical curves were calculated from Eq. (39).

Figure 24 shows that the quantity $(\partial \log a_T/\partial V_f)_T$ is not very sensitive to E* and suggests therefore that the data are not sufficiently

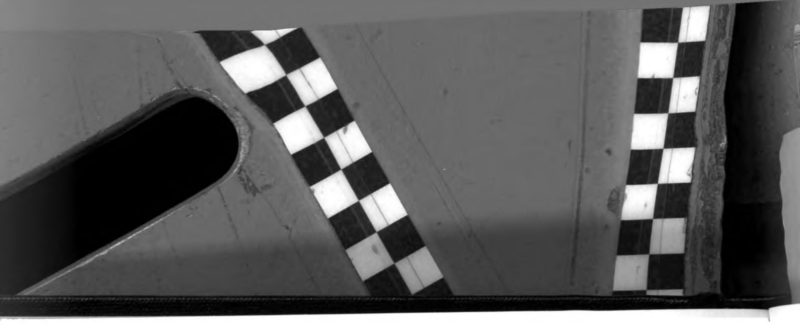

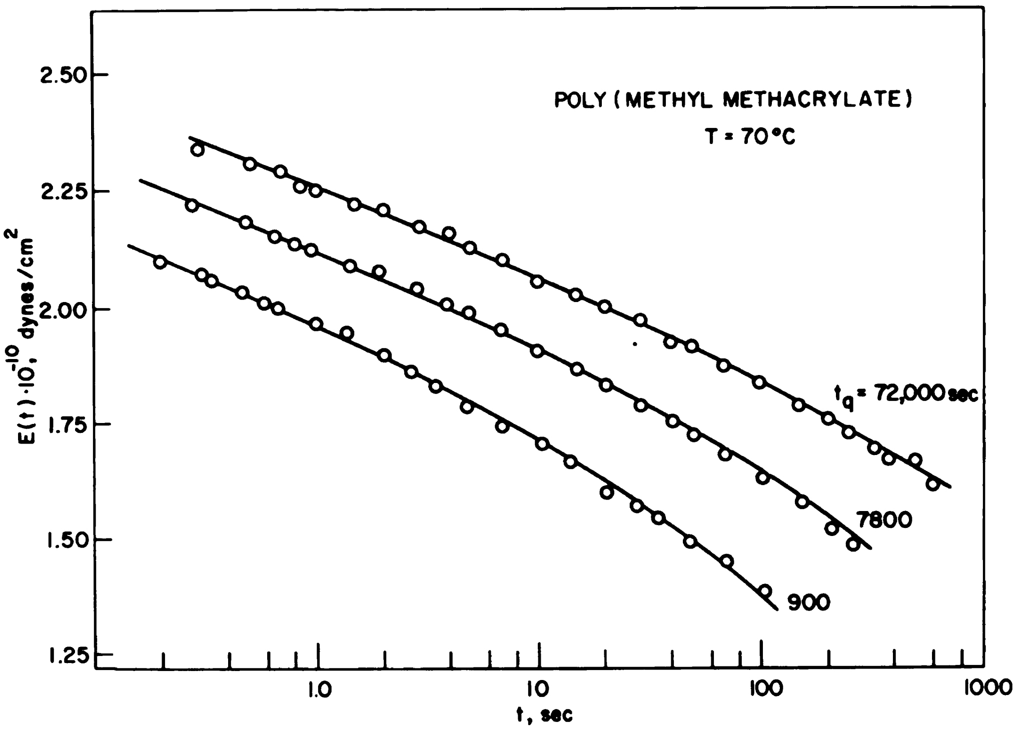

Figure 22--Series of stress-relaxation curves for PMMA for various times after quench for T = 70°C.

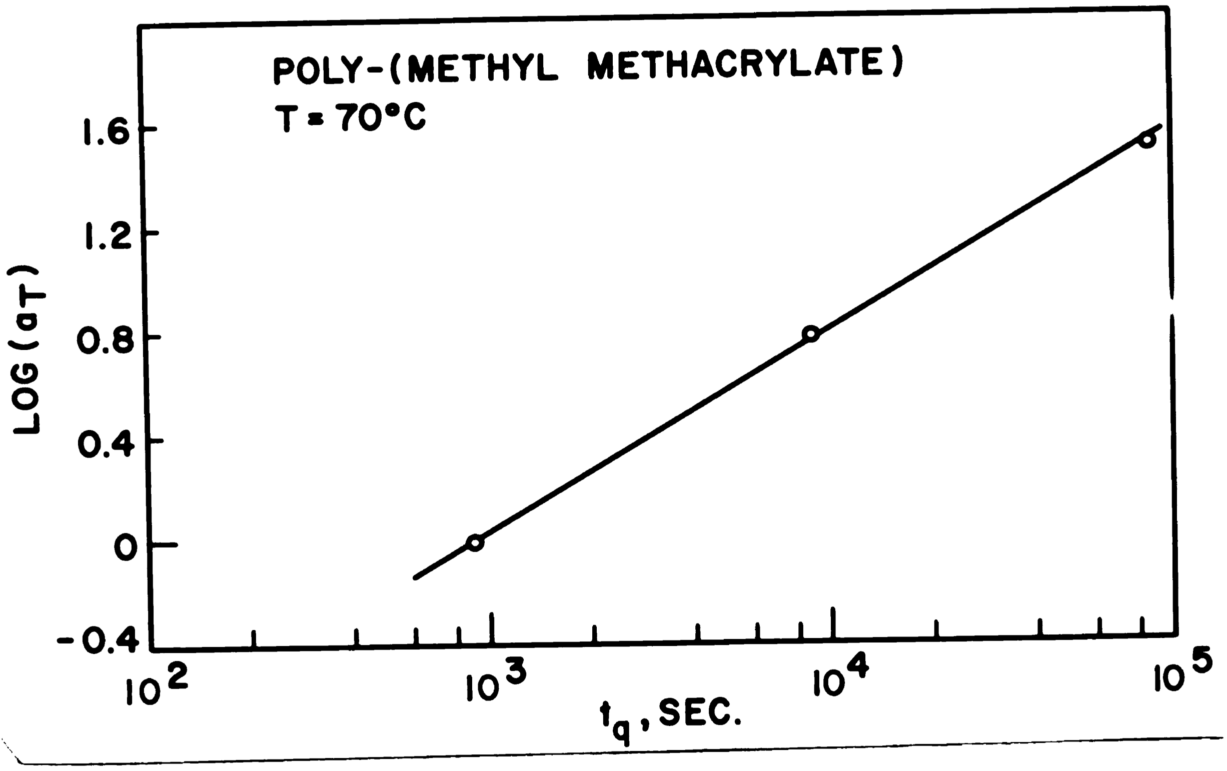

Figure 23--Log a_T of PMMA as a function of time after quench for T = 70°C.

accurate to determine the parameter. It does appear that E* lies between 0 and 25 Kcal/mole, but yield-strain data seems needed to obtain E* accurately.

TABLE 5

DEPENDENCE OF FREE VOLUME UPON TIME AFTER QUENCH

$T, ^{o}C$	$-(\partial V_f/\partial \log t_q)_T, cm^3/g \cdot 10^2$
-10	2.82
0	2.94
10	3.07
20	3.20
30	3.33
40	3.46
50	3.58
60	3.71
70	3.84
80	3.97
90	4.10
100	4.22

Equation (29) was used to fit the yield strain data for $\dot{\varepsilon}$ = 1.2% per second, and the value of T_g^* was chosen as that which gave the best fit to the data with E* = 0, 97°C. This was thought to be reasonable since the specific volume-temperature curve of Figure 7 indicates a T_g of about 94°C. Theoretical curves were calculated using T_g^* = 97°C and values of E* of 0,5,10,15,20,25,30, and 35 Kcal/mole. These are presented in Figure 25, along with the data for $\dot{\varepsilon}$ = 1.2% per second. The figure shows that E* = 20 Kcal/mole gives the best fit to the data, and this value is consistent with the range obtained by shifting the log a_T data. In the following calculations, E* will be taken as 20 Kcal/mole, and C_1, C_2, and $\Delta\alpha_f$ will be given the corresponding values from Table 4.

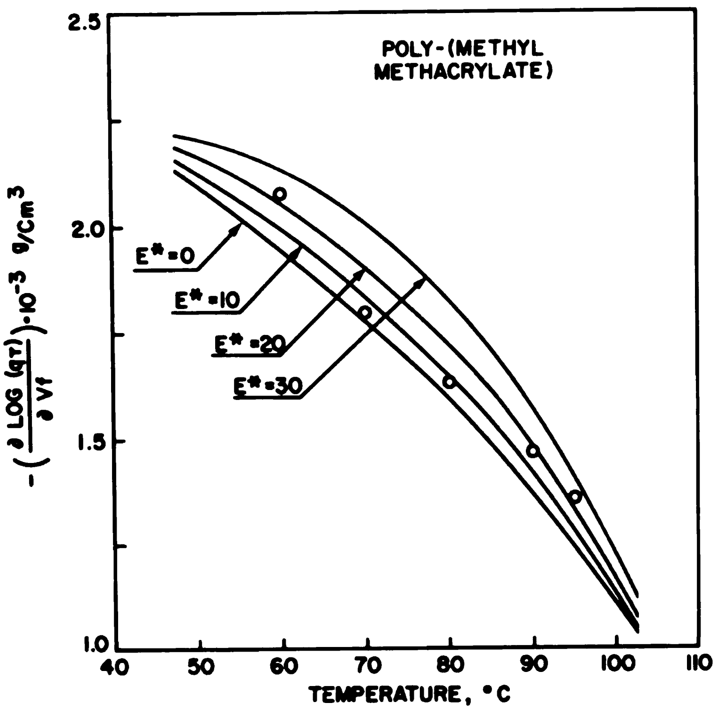

Figure 24-- $-(\partial \log a_T/\partial V_f)_T$ of PMMA as a function of temperature; points are experimental data and lines are calculated from the theory.

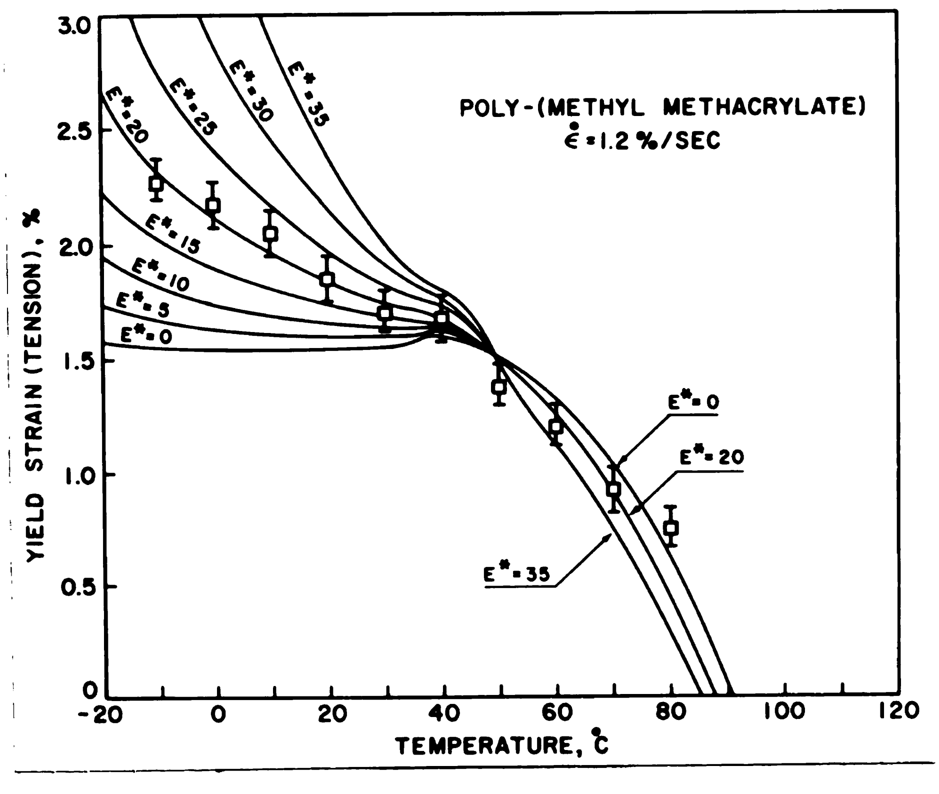

Figure 25--Yield strain of PMMA as a function of temperature for $\dot{\varepsilon}$ = 1.2%/second and theoretical curves for various values of E*.

The full set of yield strain data for all strain rates, together with the theoretical curves calculated using E* = 20 Kcal/mole are shown in Figure 26. The curves were determined by applying Eq. (29), with values of T_g^* for rates other than 1.2%/second being found from Eq. (32). Also $\dot{\varepsilon}_o$ = 1.2%/second and $T_g^*\ (\dot{\varepsilon}_o)$ = 97°C. The values of

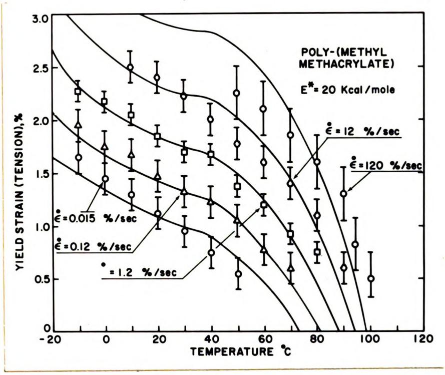

Figure 26--Yield strain of PMMA as a function of temperature and theoretical curves for E* = 20 Kcal/mole.

T_g^* are listed in Table 6, and Table 7 lists the values of $T_e(T)$ corresponding to E* = 20 Kcal/mole used in the yield-strain calculations. These values of effective temperature were obtained from T_e as determined from the log a_T data. The data for $(\partial V_f/\partial \log t_q)_T$ listed in Table 5 were used to calculate values for T_e corresponding to t_q = 1800 seconds, applicable to the yield strain data.

TABLE 6

T_g^* VALUES FOR VARIOUS STRAIN RATES

$\dot{\varepsilon}$,%/second	T_g^*,°C
0.015	93.6
0.12	95.1
1.2	97.0
12	99.1
120	101.5

TABLE 7

EFFECTIVE TEMPERATURE FOR $E^* = 20$ Kcal/mole AND $t_q = 1800$ SECONDS

T,°C	T_e,°C
-10	91.29
0	91.30
10	91.38
20	91.51
30	91.82
40	92.12
50	92.68
60	93.38
70	94.48
80	95.99
90	98.33
100	102.55

The slopes of the lines in Figure 13 represent the derivative $\partial\varepsilon_y/\partial\log t_q$. These slopes were divided by the values of $\partial V_f/\partial\log t_q$ from Table 5, to obtain experimental values for $\partial\varepsilon_y/\partial V_f$. Equation (29) was used to calculate the dependence of yield strain upon V_f, since

T_e is a function of free volume. Differentiation with respect to V_f gives

$$\frac{\partial \varepsilon_y}{\partial V_f} = \frac{-\rho}{1-2\mu}\left[\rho\Delta\alpha_f\left[T_o - C_2 - T'_e + \left[\frac{1}{C_2 + T^*_g - T_o} + \frac{E^*(T-T^*_g)}{2.303 C_1 C_2 R T^* T_g}\right]^{-1}\right] + 1\right]^{\frac{2\mu}{1-2\mu}}, \tag{40}$$

the equation which was employed to determine theoretical values of $\partial\varepsilon_y/\partial V_f$. Both theoretical and experimental results are summarized in Table 8.

TABLE 8

DEPENDENCE OF YIELD STRAIN UPON FREE VOLUME

T, °C	$-\partial\varepsilon_y/\partial V_f$,exp,g/cm^3	$-\partial\varepsilon_y/\partial V_f$,calc,g/cm^3
40	4.25	5.30
50	4.42	5.65
60	4.04	5.94
70	3.55	6.19
80	3.98	6.43
90	3.22	6.69

5.2 Relaxation Rate

Equation (33) provides the basis for calculating the dependence of relaxation rate on temperature, elongation, and free volume. Equation (25) shows that τ depends upon T_e and T, but since T_e is dependent upon temperature and free volume, as expressed by Eq. (23), Eq. (25) can be used to calculate the relations between τ and those parameters. The dependence of relaxation rate on temperature and free

volume is a result of its dependence on τ. The relaxation spectrum, $H(\tau)$, used in the calculation is a modification of a spectrum for PMMA at 40°C due to Tobolsky.[36] That spectrum was extrapolated to the $\log H(\tau) = 0$ axis, and shifted along the $\log(\tau)$ axis so that the calculated and experimental values of relaxation rate would agree at 40°C. The spectrum is shown in Figure 27. Because of the analytic intractability of Eq. (33), numerical integration was carried out using the trapezoidal rule and intervals of 0.5 on the $\log(\tau)$ axis.

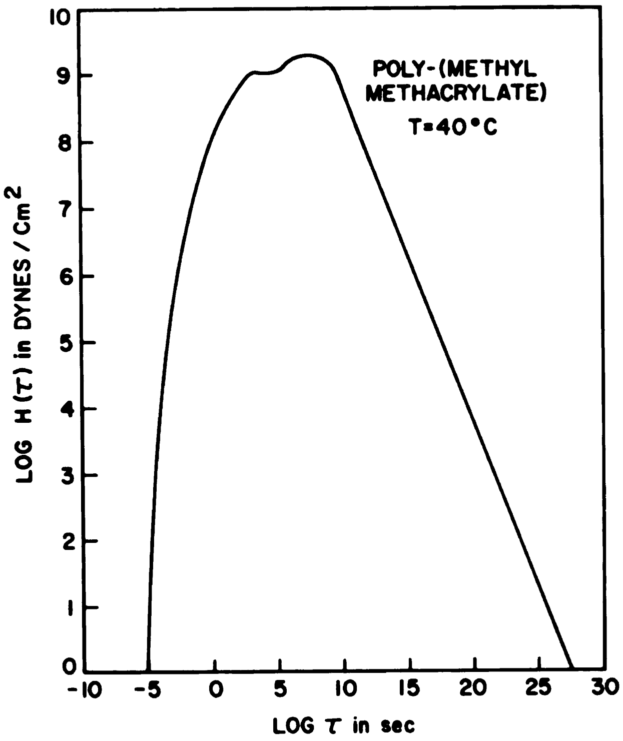

Figure 27--Relaxation spectrum used in integration of Eq. (33).

Temperature dependence of the relaxation rate was calculated using Eq. (33). For $T > T_g$ the WLF assumption, that the effect of a temperature change is to multiply all the relaxation times by the shift factor a_T, is known to hold.[13] A similar assumption will be made for the glass, however, in this case not only a change in temperature but also a change in effective temperature can cause a shift. Since τ is known to within

a constant through Eq. (25), the ratio of τ's for any two sets of values of T and T_e can be calculated. Thus, given the set of τ's for the spectrum for any one state, the τ's for any other state can be calculated. Then from Eq. (33) the relaxation rate may be obtained by numerical integration.

Since the relaxation-rate-versus-temperature data correspond to $t_q = 10^4$ seconds,[13] and since the spectrum was shifted so that theoretical and experimental relaxation rate agree at 40°C, the final spectrum should correspond to the glass at 40°C and $t_q = 10^4$ seconds. The values of $T_e(T)$ used are those for $E^* = 20$ Kcal/mole and $t_q = 10^4$ seconds.

Because the location of the spectrum on the $\log(\tau)$ axis is known for the 40°C,10^4 sec state, the position for any other state can be found by multiplying the τ's of the known state by the ratio of the τ's for the shifted and known states. For the case of temperature dependence, with t_q the same for all temperatures, we have

$$\tau(T) = \tau(40)\left[\frac{\tau(T)}{\tau(40)}\right] \tag{41}$$

or

$$\tau(T) = \tau(40)\left[\frac{\exp(E^*/RT)\exp(2.303C_1C_2/[T_e(T)-T_o+C_2])}{\exp(E^*/R\cdot 313)\exp(2.303C_1C_2/[364.3-T_o+C_2])}\right], \tag{42}$$

defining τ by Eq. (25). Equation (15) was employed to calculate $E(t)$ at $t = 7.95$ and 12.6 seconds ($\log t = 0.9$ and 1.1), and the numerical derivative obtained at each temperature. The BASIC computer program used for the relaxation rate determinations is given in the Appendix. As listed, the program is for calculation of temperature dependence. The results of the calculation are shown in Figure 28.

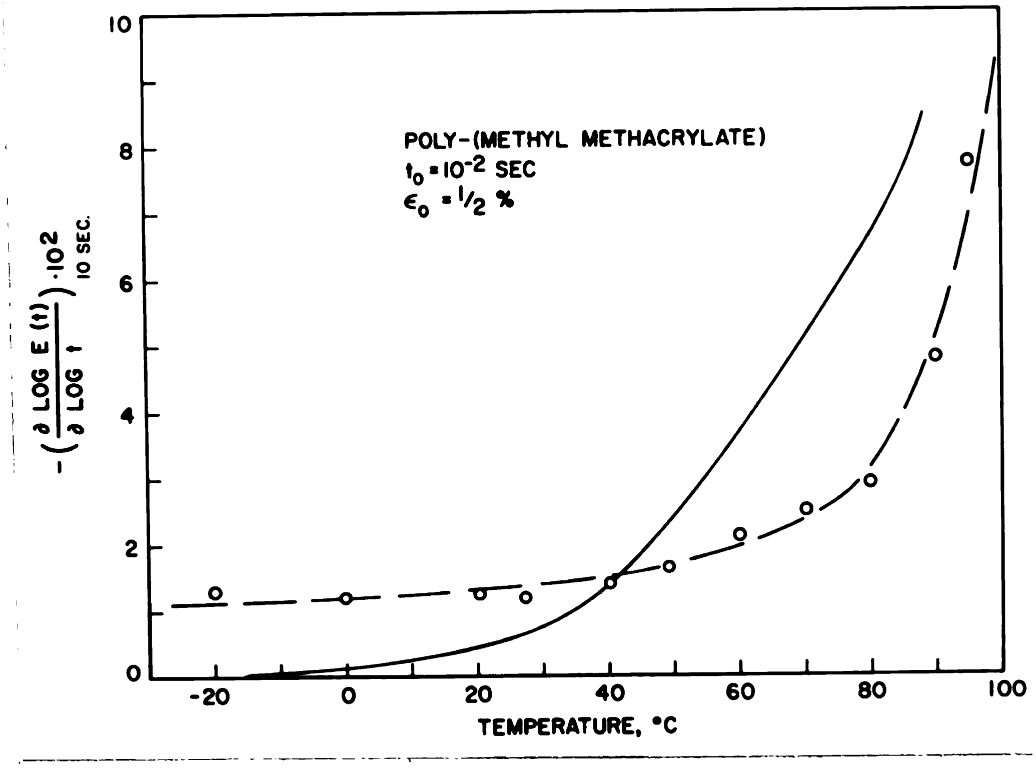

Figure 28--Ten-second relaxation rate of PMMA as a function of temperature and theoretical curve.

The dependence of relaxation rate upon elongation is determined by shifting the spectrum in a manner similar to the above. The spectrum of Figure 27 corresponds to an applied strain of 0.5%, since the relaxation-rate-temperature data, for which the spectrum was standardized, were obtained with that level of applied strain. For the specimens employed, this corresponds to an elongation of 0.033 cm.

Changes in applied elongation cause the effective temperature to change according to Eq. (26), and that expression was used to calculate T_e as a function of elongation in increments of 0.025 cm. For each value of T_e, the set of τ's was determined and the relaxation rate obtained as described above for temperature dependence. It should be noted, however, that Eq. (26) only applies prior to yield, since just to that point does μ remain constant. For the strain rate applied during

the testing, the yield point occurs at about 0.1 cm elongation, so the elongational dependence of the relaxation rate is calculated up to that value.

Because the specimens used in the experiment were not annealed and quenched, but rather used in the as-received condition, it was not possible to calculate a value for initial effective temperature. The procedure employed to initialize T_e was to choose that value which caused the theoretical and experimental relaxation rate for 60°C to agree at the first data point. The initial value for 80°C was found by adding to the 60°C value the difference in effective temperatures for 60°C and 80°C from Table 7. The values of T_e actually used are: $T_e(60) = 86.6°C$ and $T_e(80) = 89.2°C$. Calculated results, along with the experimental data are shown in Figure 29.

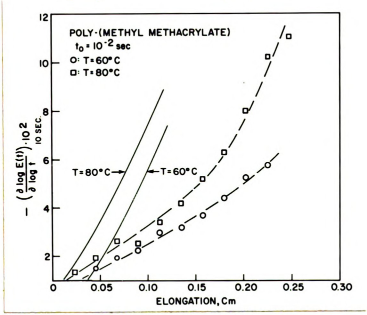

Figure 29--Ten-second relaxation rate of PMMA as a function of applied elongation and theoretical curves.

The variation of relaxation rate with time after quench, t_q, is assumed to come about as a result of nonequilibrium free volume relaxing out of the polymer. Thus, the dependence of effective temperature upon t_q is obtained from

$$\frac{\partial T_e}{\partial \log t_q}_T = \left[\frac{\partial T_e}{\partial V_f}\right]_T \cdot \left[\frac{\partial V_f}{\partial \log t_q}\right]_T = \frac{1}{\Delta\alpha_f}\cdot\left[\frac{\partial V_f}{\partial \log t_q}\right]_T \qquad (43)$$

where the values of the derivative $(\partial V_f/\partial \log t_q)_T$ are those listed in Table 5.

For each temperature the spectrum was shifted as for the previous calculations and the relaxation rate determined for various values of t_q. The results are shown in Figures 30 and 31.

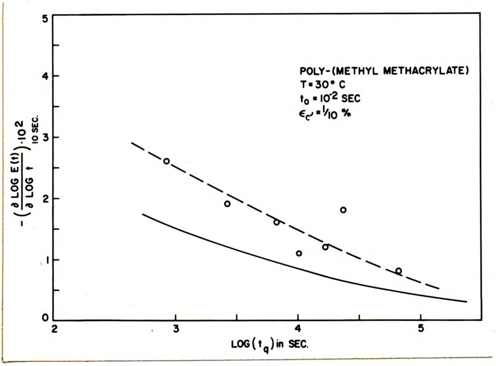

Figure 30--Ten-second relaxation rate of PMMA as a function of time after quench for T = 30°C and theoretical curve.

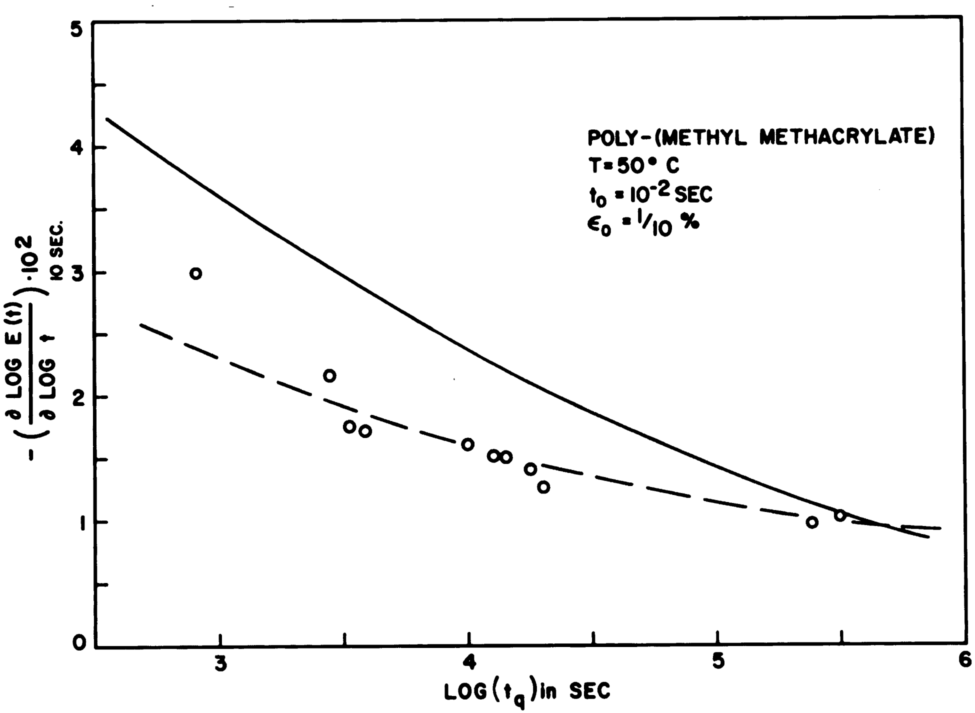

Figure 31--Ten-second relaxation rate of PMMA as a function of time after quench for T = 50°C and theoretical curve.

5.3 Direct Yield-Relaxation Relation

If yield is relaxational in nature, then, based upon the present free-volume theory and viscoelasticity theory, it should be possible to calculate a load-elongation curve from the data obtained with the tensile extension dilatometer. Equation (34), which describes stress as a function of time during tensile loading of a single Maxwell element, is rewritten for a series of elements as

$$\sigma(t) = \dot{\varepsilon}\int_{-\infty}^{\infty}\tau H(\tau)\,[1 - \exp(-t/\tau)]\,d\ln\tau. \qquad (44)$$

Using numerical integration, and shifting the spectrum according to the measured volume changes of Figure 8 and their relation to effective temperature, the stress experienced by the specimen was calculated.

Owing to the complex thermal history of the dilatometer specimens (see Appendix), comparison flexural tests to determine the effective length of the test pieces were not made. The length was simply taken as 6.6 cm, equal to that of the standard ring tensile specimens. For this value, the initial unstrained effective temperature of the specimens was calculated from the yield point using Eq. (29) with E* = 20 Kcal/mole. T_e was found to be 90°C. The unstrained volume of the specimen was taken to be 6.6A, where A is the area of the narrowest cross section. Assuming uniform deformation, the load on the specimen was calculated according to

$$\text{LOAD} = \text{STRESS}\cdot\text{VOLUME}/\text{LENGTH} \tag{45}$$

where VOLUME means the sum of the unstrained volume and the strain-induced volume, and LENGTH refers to the strained length.

In order to have a meaningful comparison of the experimental and calculated load-elongation curves, the height of the relaxation spectrum was adjusted so that the initial modulus of the calculated curve was equal to that of the experimental one. Both curves are shown in Figure 32.

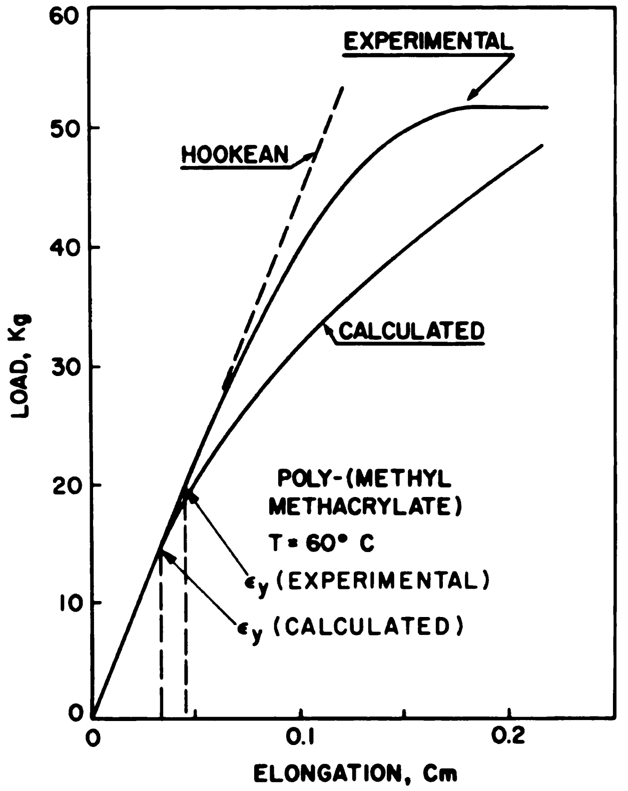

Figure 32--Experimental and calculated load-elongation curves for PMMA for T = 60°C.

6. DISCUSSION

It was stated in the introduction that glassy yield is relaxational in nature, and that the imposition of strain causes an increase in relaxation rate in much the same way that temperature causes such an increase. When the relaxation rate of the glass in the strained state reaches that value characteristic of the unstrained glass at T_g^*, yield is presumed to occur. Relaxation rate then becomes equivalent to strain rate. This qualitative description of yield was expressed mathematically by assuming that chain mobility is dependent upon two parameters, free volume and kinetic energy, and that the volume increase which accompanies applied strain corresponds in its entirety to an increase in free volume.

It can be seen from Figure 16 (relaxation rate as a function of elongation) that the rate does increase with increasing strain, and from Figure 17 (relaxation rate as a function of time after quench) that it does depend upon the specific volume of the glass in a manner consistent with the theory. Figures 12 and 14 for yield strain as a function of temperature, strain rate, and time after quench show that that parameter also behaves as predicted by the theory.

Because of the increase in relaxation rate with temperature (Figure 15), yield strain decreases with temperature. Yield strain increases with strain rate as a result of the increase in relaxation rate necessary to compete with the externally applied strain rate. The decrease in relaxation rate with decreasing specific volume causes

a corresponding increase in the applied strain needed to bring the relaxation rate of the strained glass to that level characteristic of the unstrained glass at T_g^*. The experimental data, then, qualitatively verify the description of the yield process presented in the introduction and thus the concept of the relaxational character of yield.

Figure 26 demonstrates that the mathematical theory as embodied in Eqs. (25) and (29) agrees with the data for yield strain as a function of temperature and strain rate only strain rates within one decade of the reference rate. At low and high rates the agreement is marginal.

As indicated in Table 8, experiment and theory are not in good agreement for the specific volume dependence of yield strain. The data and theoretical values trend in opposite directions with increasing temperature. In part at least, this may be a result of inaccuracies in the data, as the scatter (shown in Figure 14) is substantial.

Figures 28-31 clearly show the theory to be unsatisfactory for quantitative calculation of relaxation rate as a function of temperature, elongation, or time after quench. Qualitatively the theory is successful; it predicts changes in relaxation rate with the parameters which are in the same direction as experimental results. But quantitatively, it predicts a greater dependence upon temperature and elongation than is experimentally observed. As regards time after quench, in the case of 30°C the experimental dependence is greater than predicted by theory, whereas for 50°C the opposite is true.

The theory is partially successful when used to calculate a load-elongation curve from measured volume changes. Figure 32 shows that the calculated curve, though not coincident with the experimental one, does exhibit a distinct yield point at an elongation of 0.033 cm.

The experimental yield point occurs at 0.045 cm. However, the calculated curve predicts a greater change of load with elongation past the yield point than is actually observed.

The fact that a yield point can be calculated using actual volume measurements indicates that the theory is consistent with the yield-relaxation model. And though it provides good evidence for accepting the yield-relaxation idea, it does not prove such a relation to be fact. Likewise, the agreement between theory and experiment for yield strain and relaxation rate qualitatively indicates that yield is relaxational in nature, but cannot be considered proof. To provide such proof, it would be necessary to establish the equivalence between relaxation rate and strain rate at the yield point.

The basis of the derivation of Eq. (29) for yield strain as a function of temperature and effective temperature is that the critical transitional probability can be calculated for an unstrained specimen when $T \approx T_g$. This implies that for yield at temperature T, τ_T is equivalent to τ_{T_g}, and thus that the relaxation rate of the glass at the yield point is equal to the relaxation rate of an unstrained specimen at T_g. Such an implication can be checked, on a macroscopic scale, using the data previously presented.

Taking as an example the particular specimen whose load-elongation curve is shown in Figures 8 and 32 (the dilatometer specimen for 60°C), we find the yield elongation to be 0.045 cm. With an effective length of 6.6 cm, yield strain is 0.7%. The elongation rate of 10^{-3} cm/second indicates that yield occurred at $t = 45$ seconds, and this elongation rate corresponds to a strain rate of 0.015%/second, which from Table 6 gives a T_g^* value of about 94°C. Figure 4 shows that the 45-second

relaxation rate for a specimen strained 0.5% at 94°C is approximately 14.0×10^{-2}.

The relaxation rate for the unstrained state can be approximated from Figure 16. For 60°C and 80°C, the slopes of the relaxation rate-elongation curves are 2.1×10^{-1} cm^{-1} and 2.6×10^{-1} cm^{-1} respectively. Extrapolated linearly, a value of 3.0×10^{-1} cm^{-1} is obtained for 94°C. A strain of 0.5% for the specimens of Figure 4 corresponds to an elongation of 0.033 cm for the dilatometer specimen. By substracting the relaxation rate increase due to the elongation of 0.033 cm, the relaxation rate of an unstrained specimen at 94°C can be calculated to be about 13×10^{-2}.

Figure 4 shows that the 45-second relaxation rate for 60°C and 0.5% strain is 4×10^{-2}. Adding the rate attributable to the difference in strain between the 0.5% of Figure 4 and the 0.7% of the dilatometer specimen, the relaxation rate of the specimen at yield is about 4.5×10^{-2}. Therefore, this rough calculation shows that for 60°C the relaxation rate of a specimen at the yield point and the rate of an unstrained specimen at T_g^* differ by about a factor of three. This is approximately the same difference in rate between 60°C and 94°C shown in the data of Figure 15, which was taken at equal values of applied strain for all specimens. On a macroscopic scale, then, relaxation rate-strain rate equivalence appears not to be valid. This does not disprove the model on a microscopic scale, however, since relaxation rate-strain rate equivalence could be reached in localized regions of the specimen as a result of stress concentrations near inhomogeneities.

The failure of the theory adequately to describe relaxation, while working fairly well for yield strain, may arise as a result of

several factors. First, it is not surprising that the poorest agreement is achieved in the description of relaxation rate. Yield strain according to Eq. (29) is approximately proportional to $(T_g^* - T_e)^3$, whereas relaxation rate is proportional to $\exp(-t/\tau)$, where τ itself varies exponentially with $1/T_e$. Therefore, any inaccuracies in effective temperature which could arise as a result of errors in measuring log a_T or volume--or in the determination of E*--have a much greater effect upon relaxation rate than upon yield strain.

The numerical integration and the subsequent differentiation of Eq. (33) are also potential sources of error. Integration over equal intervals along the log τ axis means that along the τ axis the intervals become very large. Numerical differentiation also may lead to error, since by its nature differentiation tends to accentuate inaccuracies, rather than smooth them out.

The most probable cause of the differences noted, however, is the failure of Eq. (25) to describe the dependence of relaxation times upon free volume in the glassy state. Such a failure could come about simply because the equation is not applicable to the glassy state, or it could arise from the assumption that only free volume and temperature control molecular mobility. In any case, it is apparent that the use of Eq. (25) to shift the spectrum of relaxation times results in calculating a greater change in relaxation rate than is observed experimentally.

One other deficiency exists in the free-volume treatment--the failure of the theory to describe the yield process in stress fields other than those with a tensile component. No volume increase accompanies compressive strain, for instance; instead, the volume decreases. Therefore, assuming uniform compressive deformation, the

free-volume theory predicts that the glass will never yield, which is not the case.[11,37]

The first explanation of this apparent inconsistency is that proposed by Volkov.[38] He has suggested that as a result of inhomogeneities within a material, even though the bulk stress field is compressive, regions around such inhomogeneities are in tension, and thus that failure and yield, originating in these areas, actually occur in tension. Thomason[39] has done some work on steel which would appear, qualitatively, to bear out this mechanism. It is also a possibility, of course, that two separate mechanisms are involved in tensile and compressive yield, so that the free volume concept holds in tension, whereas some other mechanism obtains in compression.

The final possibility is that volume itself does not control glassy relaxation, but only reflects some controlling thermodynamic parameter. One can envision a mechanism whereby the work term of an entropy equation, which is directly related to the dilational component of the applied stress, would promote yield in tension but retard it in compression. This possibility appears to be particularly strong in light of results which show that the yield stress in compression for PMMA glass is 15-20% higher than in tension.[11,37]

The ultimate objective of any investigation of yield should be a generalized yield criterion applicable to any stress field. Free volume, as it now stands, cannot be considered as such a criterion. What is needed is a series of biaxial and multiaxial stress-strain measurements in which initial yield point is measured. Other workers[10,11] have made biaxial yield measurements, but all have been of the upper yield stress, or the stress required to craze the material. Such a

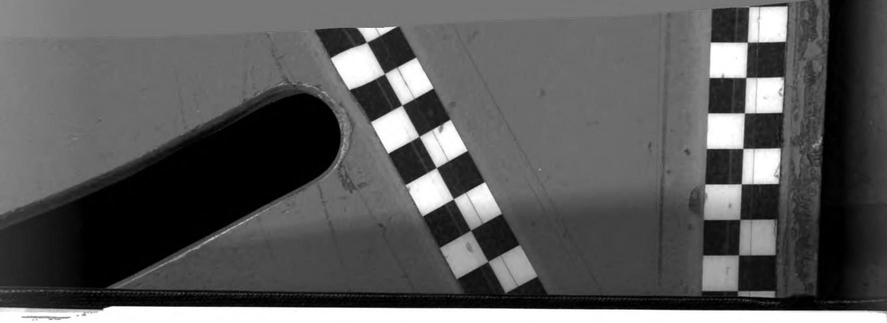

series of measurements of initial yield point would serve as a starting point for the determination of a generalized yield criterion for polymeric glasses.

7. CONCLUSIONS

The modified free-volume theory is useful for predicting initial tensile yield strain, defined as the strain at the proportional limit of the load-elongation curve, for strain rates within one decade of the reference rate. Agreement is marginal for rates which differ from the reference rate by more than a factor of ten. The theory, although applicable for qualitative purposes, is not successful quantitatively for calculating the dependence of initial yield strain upon time after quench to the glassy state from a temperature greater than T_g.

The theory is inadequate for quantitative calculations of relaxation rate. In general, for the dependence of rate upon temperature, applied elongation, and time after quench, the theory predicts greater changes than are observed experimentally, although qualitative agreement is found.

Whether glassy yield of amorphous polymers is a relaxational phenomenon, as is the glass transition, is still unresolved. Although all of the data presented here are consistent with such a relationship, none offer positive proof. If relaxation-rate/strain-rate equivalence is realized in the glass, it must occur locally, since on a macroscopic scale the rates do not agree.

Therefore, though the modified free-volume theory may serve as a starting point for describing the yield and relaxation behavior of PMMA

(and perhaps other amorphous thermoplastic polymer glasses), considerable additional refinement would be necessary for quantitative applicability.

LIST OF REFERENCES

LIST OF REFERENCES

1. J. S. Lazurkin, J. Poly. Sci. 30, 595 (1958).
2. R. E. Robertson, J. Chem. Phys. 44, 3950 (1966); Polymer Preprints 8, No. 2, 1501 (1967).
3. R. E. Robertson, Appl. Poly. Symposia 7, 201 (1968).
4. W. Holzmuller, Kolloid Z. 155, 110 (1957).
5. M. Goldstein, J. Poly. Sci. B4, 87 (1966)
6. J. D. Ferry and R. A. Stratton, Kolloid Z. 171, 107 (1960)
7. S. Newman and S. Strella, J. Appl. Poly. Sci. 9, 2297 (1965).
8. M. H. Litt and A. V. Tobolsky, J. Macromol. Sci. 9, 433 (1967).
9. M. H. Litt, P. J. Koch and A. V. Tobolsky, J. Macromol. Sci. B1, 587 (1967).
10. S. S. Sternstein, L. Ongchin and A. Silverman, Appl. Poly. Symposia 7, 175 (1968).
11. W. Whitney and R. D. Andrews, J. Poly. Sci. C16, 2981 (1967).
12. D. H. Ender, J. Macromol. Sci., in press.
13. K. C. Rusch, J. Macromol. Sci. B2(2), 179 (1968).
14. W. Kauzmann, Chem. Rev. 43, 219 (1948)
15. J. H. Gibbs and E. A. DiMarzio, J. Chem. Phys. 28, 373 (1958); 28, 807 (1958); J. Poly. Sci. 40, 121 (1959); Ibid, A1, 1417 (1963).
16. K. C. Rusch, unpublished data.
17. M. L. Williams, R. F. Landel and J. D. Ferry, J. Am. Chem. Soc. 77, 3701 (1955).
18. G. Adam and J. H. Gibbs, J. Chem. Phys. 43, 139 (1965).

LIST OF REFERENCES (CONT.)

19. L. C. E. Struik, Rheolo. Acta 5, 303 (1966).

20. A. K. Doolittle, J. Appl. Phys. 22, 1471 (1951); A. K. Doolittle and D. B. Doolittle, J. Appl. Phys. 28, 901 (1957).

21. M. H. Cohen and D. Turnbull, J. Chem. Phys. 31, 1164 (1959); D. Turnbull and M. H. Cohen, J. Chem. Phys. 34, 120 (1961).

22. S. N. Glasstone, K. Laidler and H. Eyring, The Theory of Rate Processes. New York: McGraw-Hill, 1941.

23. H. P. Weymann, Kolloid Z. 181, 131 (1962).

24. P. B. Macedo and T. A. Litovitz, J. Chem. Phys. 42, 245 (1965).

25. J. C. Maxwell, Phil. Mag. 35, 134 (1868).

26. F. S. C. Chang, High Speed Testing, Vol. IV 37, Interscience (1964).

27. G. Adam and J. H. Gibbs, J. Chem. Phys. 43, 139 (1965).

28. T. G. Fox and P. J. Flory, J. Appl. Phys. 21, 581 (1950).

29. T. L. Smith, J. Poly. Sci. 20, 89 (1956); 22, 99 (1958).

30. F. Beuche, J. Appl. Phys. 22, 603 (1954).

31. J. D. Ferry, Viscoelastic Properties of Polymers. New York: John Wiley & Sons, Inc., 1961.

32. D. C. West, Expl. Mech. 4, 185 (1964).

33. A. G. Fedorenko and B. N. Pashin, Plast. Massy 11, 46 (1965).

34. V. J. Koppelman, Rheol. Acta 1, 20 (1958).

35. A. J. Kovacs, R. A. Stratton and J. D. Ferry, J. Phys. Chem. 67, 152 (1963).

36. A. V. Tobolsky, Properties and Structure of Polymers. New York: Wiley, 1960.

37. P. Beardmore, Phil. Mag. 19, 389 (1969).

38. S. D. Volkov, Statisticheskoya Teoriya Prochnosti, (Mashgiz), 1960.

39. P. F. Thomason, Int. J. Mech. Sci. 11, 187 (1969).

40. T. L. Smith, Trans. Soc. Rheol. III, 113 (1959).

APPENDIX

A. DILATOMETER

The present dilatometer is similar in design to one employed by Smith[40] to make volume measurements on rubber. Figure 33 is a schematic drawing of the instrument. It consists of a cylindrical barrel (A)

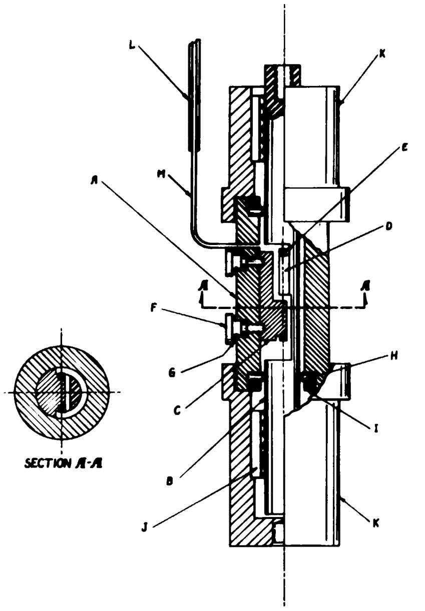

Figure 33--Schematic drawing of tensile-extension dilatometer.

through which extends a round shaft (B). The shaft has a notch cut out which mates with a matching piece (C) bolted inside the barrel. Both shaft and matching piece are fitted with carriers (D) by which the specimen (E) (Figure 34) is held. The notch and the matching piece are sized to allow the shaft a travel of 1.6 cm relative to the

[illegible]

[illegible]

Figure [illegible] dilatometer.

through [illegible] (Figure [illegible]). The [illegible] has a notch cut out which [illegible] (2) bolted inside the barrel. Both shoul[illegible] fitted with carriers (5) on which the specimen (6) [illegible] is held. The notch and the matching piece are sized to allow the [illegible] a travel of 1.5 mm relative to the matching piece and barrel. The bolts (F) which fix the matching piece inside the barrel are sealed with rubber 'O' rings (G), and the ends of the barrel through which the shaft extends are sealed with special teflon gaskets (H) which are secured by threaded rings (I). The shaft is held parallel to the barrel by ball bushings (J), mounted in end caps (K).

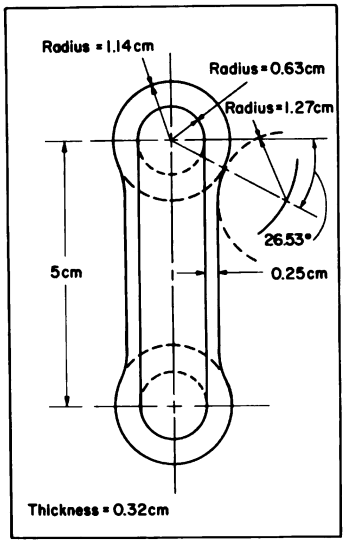

Figure 34--Tensile-extension dilatometer specimen.

Volume changes are measured using a 0.1-cm diameter precision-bore capillary (L) in which the height of the confining fluid, mercury, is followed. The capillary is connected to the barrel by a short length of 0.13-cm I.D. teflon tubing (M). Mercury was chosen as the fluid owing to the inertness of polymer glasses with respect to it. All metal parts of the instrument were fabricated of ASA 1020 steel to avoid amalgamation of the mercury with alloying elements.

moulding glass [illegible]

inside the barrel [illegible]

the barrel [illegible]

within gate [illegible]

is held [illegible]

page 10) [illegible]

Figure [illegible]

[illegible]

collimator [illegible]

follows. [illegible]

of 0.13 cm [illegible]

owing to the [illegible]

metal parts of [illegible]

amalgamation of [illegible]

Calibration of the dilatometer in the absence of a specimen showed a reproducible volume change of $-8 \cdot 10^{-4}$ cm^3, attributed to deformation of the teflon gaskets, which was taken into account in all testing.

B. EXPERIMENTAL PROCEDURE FOR DILATOMETER

The procedure followed in specimen preparation and testing is outlined below.

1. Anneal specimen for one hour at 130°C.
2. Quench specimen to room temperature between steel plates and hold for five minutes (thermal equilibrium is established within two minutes).
3. Assemble dilatometer with specimen.
4. Evacuate dilatometer to 10^{-5} mm Hg.
5. While still under vacuum, fill dilatometer with mercury, then open to atmospheric pressure.
6. Mount instrument on test machine within temperature chamber and allow thermal equilibrium to be established (about three hours). Because of the need to assemble and fill the instrument then bring it to the test temperature, the thermal history of the specimens is not well defined and is different for each test temperature.
7. Carry out test.

The machine used to extend the specimens is an MTS closed-loop, electro-hydraulic testing machine. The temperature was controlled by enclosing the dilatometer in a chamber capable of holding temperature constant to within 0.25°C. Because of the large mass of the dilatometer and the small oscillations of the chamber temperature, the specimen temperature remained constant once established. Testing was done at a linear rate of 10^{-3} cm/second.

During extension the height of the mercury column was followed by means of a cathetometer telescope instrumented with a D.C. position

transducer[*] which allowed recording volume changes as small as 10^{-6} cm^3. Two recorders were employed, one for each of the two plots obtained: load versus displacement, and mercury height versus displacement.

---

[*] G. L. Collins Co. model number SS205.

C. DILATOMETER AND HYSTERESIS DATA

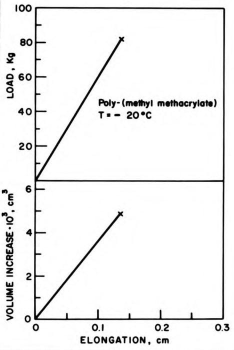

Figure 35--Tensile-extension dilatometer data for PMMA for T = -20°C.

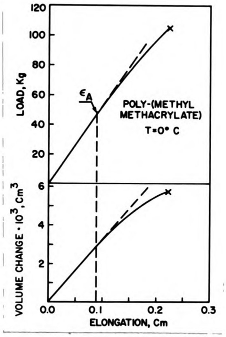

Figure 36--Tensile-extension dilatometer data for PMMA for T = 0°C.

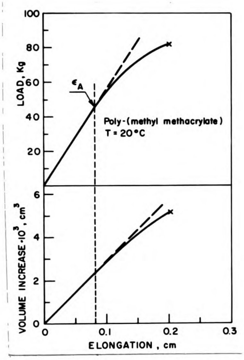

Figure 37--Tensile-extension dilatometer data for PMMA for T = 20°C.

Figure 36--[illegible] for 7004 for T = 20°C.

Figure 37--[illegible] area for 7004 for T = 25°C.

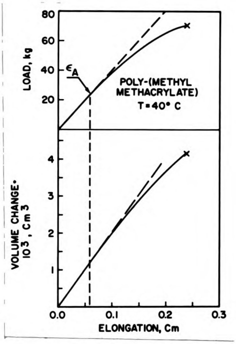

Figure 38--Tensile-extension dilatometer data for PMMA for T = 40°C.

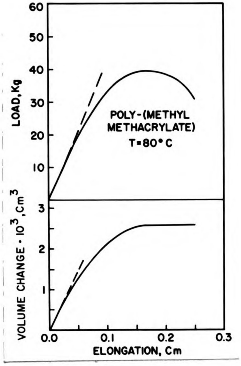

Figure 39--Tensile-extension dilatometer data for PMMA for T = 80°C.

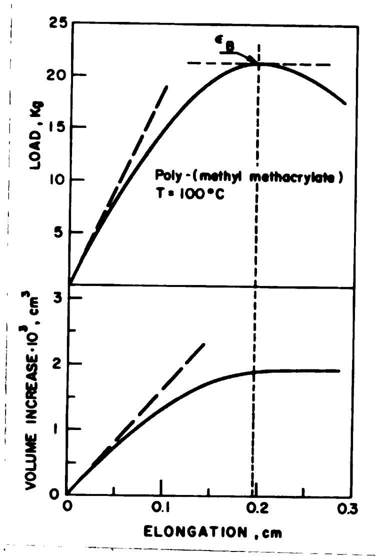

Figure 40--Tensile-extension dilatometer data for PMMA for T = 100°C.

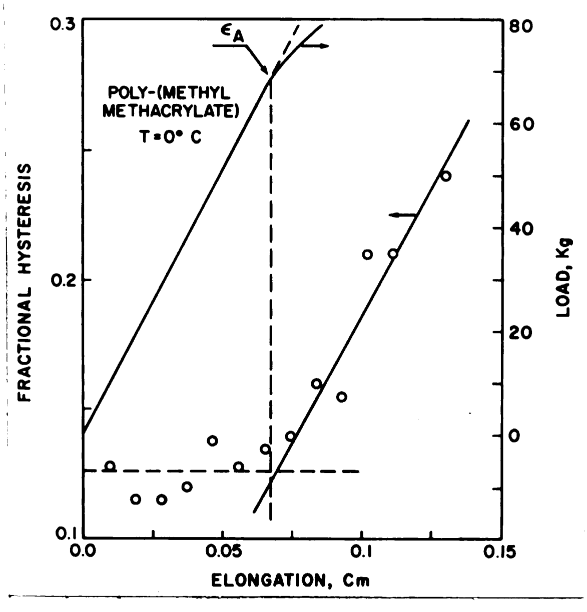

Figure 41--Fractional hysteresis data for PMMA for T = 0°C.

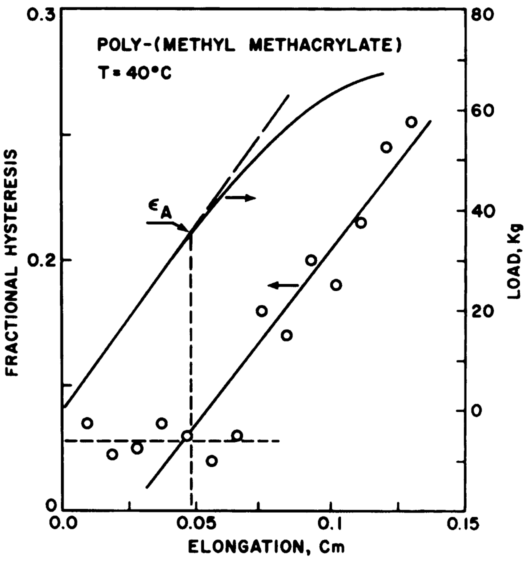

Figure 42--Fractional hysteresis data for PMMA for T = 40°C.

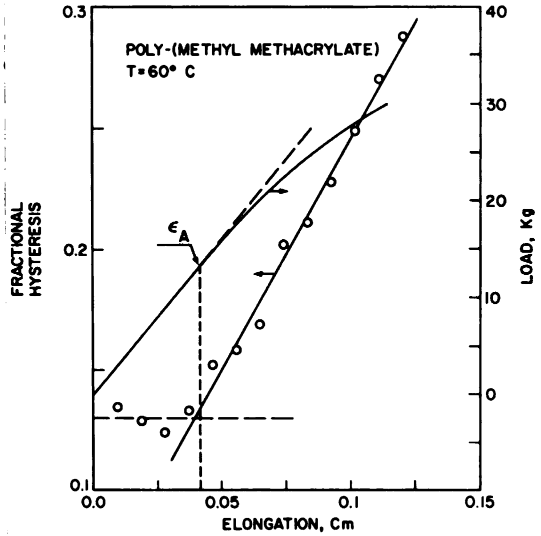

Figure 43--Fractional hysteresis data for PMMA for T = 60°C.

D. BASIC PROGRAM R-RATE USED FOR RELAXATION RATE CALCULATION-TEMPERATURE DEPENDENCE

```
100 REM THIS PRØGRAM CALCULATES THE TEMPERATURE DEPENDENCE ØF
110 REM THE TEN-SECØND RELAXATIØN RATE FØR PØLYMETHYLMETHACRYLATE
120 REM GLASS ACCØRDING TØ THE MØDIFIED FREE VØLUME THEØRY.
130 DIM A(20),B(20),E(20),H(20),L(20),T(20)
140 LET X = 5.5
150 LET T0 = 105 + 273
160 LET E1 = 20
170 LET R = 1.99E-3
180 LET C1 = 12.08
190 LET C2 = 39.8
200 FØR I = 1 TØ 11
210 READ T(I)
220 LET T(I) = T(I) + 273
230 NEXT I
240 FØR I = 1 TØ 66
250 READ H(I)
260 LET H(I) = 10↑H(I)
270 NEXT I
280 FØR I = 1 TØ 11
290 LET T1 = (I-2)*10 + 273
300 LET L(I) = E1/(R*T1) + 2.303*C1*C2/(T(I)-T0+C2)
310 NEXT I
320 PRINT "TEMPERATURE","RELAXATIØN RATE"
330 PRINT
340 FØR I = 1 TØ 11
350 LET T1 = (I-2)*10 + 273
360 FØR J = 1 TØ 2
370 LET T3 = 7.95
380 IF J = 1 THEN 400
390 LET T3 = 12.6
400 LET A(J) = 0
410 FØR K = 1 TØ 65
420 LET T2 = (K/2-X)* LØG(10) + L(I) - L(6)
430 LET T4 = (K/2-X+0.5)*LØG(10) + L(I) - L(6)
440 LET T2 = EXP(T2)
450 LET T4 = EXP(T4)
460 LET H1 = (H(K)+H(K+1))/2
470 LET A(J) = A(J) + H1*EXP(-2*T3/(T2+T4))*(LØG(T4)-LØG(T2))
480 NEXT K
490 NEXT J
500 PRINT T1-273,LØG(A(2)/A(1))/LØG(12.6/7.95)
510 NEXT I
520 DATA 90.6,90.6,90.65,90.75,91.04,91.3,91.83,92.5,93.58,95.05,97.36
530 DATA 0,2,3.6,4.65,5.55,6.18,6.7,7.1,7.48,7.76,8.04,8.26,8.45,8.62
540 DATA 8.77,8.91,9.03,9.04,9.05,9.06,9.08,9.12,9.22,9.27
550 DATA 9.3,9.31,9.29,9.25,9.17,9,8.75,8.5,8.25,8.0,7.75,7.5
560 DATA 7.25,7.0,6.75,6.5,6.25,6.0,5.75,5.5,5.25,5.0,4.75,4.5,4.25
570 DATA 4.0,3.75,3.5,3.25,3.0,2.75,2.5,2.25,2.0,1.75,1.5,1.25,1.0
580 DATA 0.75,0.5,0.25,0
590 END
```

EXPLANATION OF SYMBOLS USED IN R-RATE

X	$\log \tau$ shift necessary to cause agreement between experimental and theoretical relaxation rate at $\tau = 40°C$.
TO	T_o,°K
E1	E^*
R	gas constant
C1,C2	C_1, C_2
T(I)	$T_e(T)$, °K, for $t_q = 10^4$ seconds
H(I)	$\log H(\tau)$
T1	T, °K
T2,T4	$\ln \tau$ and $\ln (\tau + 0.5)$ (lines 420, 430) τ and $\tau + 0.5$ (lines 440, 450)
A(J)	$E(9.9)$ and $E(10.1)$ for $J = 1, 2$

MICHIGAN STATE UNIVERSITY LIBRARIES
3 1293 03082 9794